

Dynamic Earth

Plates, Plumes and Mantle Convection

GEOFFREY F. DAVIES

Australian National University



CAMBRIDGE
UNIVERSITY PRESS

(SG)
QE509
.4
D38
1999

PUBLISHED BY THE PRESS SYNDICATE OF THE UNIVERSITY OF CAMBRIDGE
The Pitt Building, Trumpington Street, Cambridge, United Kingdom

CAMBRIDGE UNIVERSITY PRESS

The Edinburgh Building, Cambridge CB2 2RU, UK www.cup.cam.ac.uk
40 West 20th Street, New York, NY 10011-4211, USA www.cup.org
10 Stamford Road, Oakleigh, Melbourne 3166, Australia
Ruiz de Alarcón 13, 28014 Madrid, Spain

© Cambridge University Press 1999

This book is in copyright. Subject to statutory exception
and to the provisions of relevant collective licensing agreements,
no reproduction of any part may take place without
the written permission of Cambridge University Press.

First published 1999

Printed in the United Kingdom at the University Press, Cambridge

Typeset in Times 10½/13pt, in 3B2 [KW]

A catalogue record for this book is available from the British Library

Library of Congress Cataloguing in Publication data

Davies, Geoffrey F. (Geoffrey Frederick)

Dynamic earth : plates, plumes, and mantle convection/ Geoffrey F. Davies.
p. cm.

Includes bibliographical references.

ISBN 0 521 59067 1 (hbk.). – ISBN 0 521 59933 4 (pbk.)
1. Earth–Mantle. 2. Geodynamics. I. Title.

QE509.4.D38 1999
551.1'16–dc21 98–51722 CIP

ISBN 0 521 59067 1 hardback

ISBN 0 521 59933 4 paperback

CHAPTER 6

Flow

The flow of viscous fluids traditionally has not received a lot of attention in geology and geophysics curricula. The discussion of mechanics more usually focusses on elasticity and brittle fracture, with which the propagation of seismic (elastic) waves and faulting of the crust and lithosphere may be considered. The formation of folds and other kinds of distributed deformation receives some attention in structural geology, but many geologists still may not be very familiar with the mechanics of fluids. The text by Turcotte and Schubert [1] has gone a considerable way towards filling this gap, but fluid flow is so fundamental to mantle convection that it is worth developing here. By doing this I can focus the development on the particular things needed to treat mantle convection, and I can also present it at a range of mathematical levels, from the simplest possible to some more advanced aspects.

To guide readers, some of the sections are marked *Intermediate* or *Advanced*. These labels indicate the mathematical level. The essence of the chapter can be obtained just from the unlabelled sections (6.1, 6.7, 6.8.1, 6.9, 6.10). The important concepts and results are presented in those sections with minimal mathematics. The intermediate sections include mathematical formulations of stress, strain rate, viscosity and the equations governing slow flow of viscous fluids. These should not be too challenging, though some practice may be required if the notation is unfamiliar. A couple of sections summarise more advanced results that have particular relevance here, for those who may wish to see them.

It is always useful to begin with the simplest mathematical treatment that can capture a piece of physics, because then the physical concepts are the least obscured by the mathematics. This may suffice for those who want to get a clear understanding of mantle convection but who do not aspire to make any contributions to the subject themselves. For those who do aspire to go

further, it is still essential to get a clear understanding of the physical concepts before proceeding to more advanced levels. Thus I begin this chapter by introducing the ideas of stress, strain, strain rate and viscosity in examples that are very simple but that permit the basic ideas and relationships to be appreciated. The basic equations of force balance and conservation of mass can also be introduced in this simple context.

These topics are then repeated, at an intermediate level, in a way that allows two- and three-dimensional problems to be treated. The equations become much messier-looking in these cases, but a concise notation retrieves a lot of the simplicity of the simple case. This ‘subscript notation’ may be unfamiliar to some, but the form of the equations closely parallels the simple cases, so a bit of practice with the notation is well worth the effort.

Some particular kinds of flow are then presented, the examples chosen to be relevant to mantle convection. Some of these are fairly simple, and some are more advanced. The latter are clearly marked, and those who wish may avoid them without sacrificing understanding of later chapters. It is not my intention here to present a comprehensive treatment of mantle flow, but rather to present some particularly pertinent examples, some of which are not readily accessible outside specialist fluid dynamics texts.

More detailed treatments of mantle flow often require numerical modelling. I do not present anything on numerical methods here because my focus is on developing a physical understanding in a way that is accessible to as wide an audience as possible. Analytical solutions are the most useful in this regard, because they reveal the way the fluid behaviour depends on parameters and material properties. The results of some numerical models will nevertheless be used in later chapters because known analytical solutions do not approach the realism required to demonstrate some key aspects of the behaviour of the mantle system.

This rather long chapter concludes with two sections on the mechanical properties of the mantle and crust. The first (6.9) outlines how observations of post-glacial rebound have been used to derive constraints on mantle viscosity. The second (6.10) considers the *rheology* of rocks more generally, rheology being the science of how materials respond to an applied stress. This includes brittle failure, which is characteristic of the lithosphere and central to the distinctive character of mantle convection. It also includes the dependence of viscosity on temperature and its possible dependence on stress (more correctly referred to as nonlinear rheology).

6.1 Simple viscous flow

In mechanical terms, a fluid is a material that can undergo an unlimited amount of deformation. A solid, on the other hand, may deform to a small extent, but it will break if you try to deform it too much. Another distinction is that many solids will deform only by a certain amount under the action of a particular force, and then return to their original shape if you stop applying that force. Such materials are called elastic. On the other hand, a fluid will keep deforming as long as a force is applied to it, and if the force is removed it will simply stop deforming, without returning to its original shape.

These distinctions are often very clear in our common experience, but in some circumstances they are not so clear. Thus, for example, some metals are elastic under the action of a small force, but yield and permanently deform if you apply a larger force. Malleable wire is a familiar example. A metal deforming permanently is behaving more like a fluid. The tendency to behave more like a fluid is enhanced in many materials if we heat them, and metals again provide a familiar example. Even when a material is solid for all practical purposes, it may be undergoing very slow deformation, so that we can consider it to be a fluid over hundreds or millions of years. We mentioned the example of glass in Chapter 2.

A *linear viscous fluid* is a material whose rate of deformation is proportional to the applied force. We will look here at how we can quantify that statement. I included the term ‘linear’ in the statement because in more general fluids the rate of deformation may be a more complicated function of the applied force. Linear viscous fluids are also known as *Newtonian* fluids. Strictly speaking, the term ‘viscous’ applies to materials in which the proportionality is linear, although the term is sometimes used more loosely. More general behaviour, such as that of malleable wire, is called variously *ductile*, *malleable* or *nonlinear*. Strictly speaking, ductile refers to materials with sufficient strength under tension that they can be stretched or drawn. Malleable would be a more appropriate term for many geological materials, but the term ductile is commonly used.

In order to quantify our definition of a viscous fluid, we need ways to characterise deformation and applied force. We can do this in the very simple situation depicted in Figure 6.1a. This shows a layer of fluid between two plates. It may help to think of the fluid being ‘stiff’, ‘thick’ or ‘gooey’ like honey or treacle (molasses). The top plate is moving to the right with velocity V , and the bottom

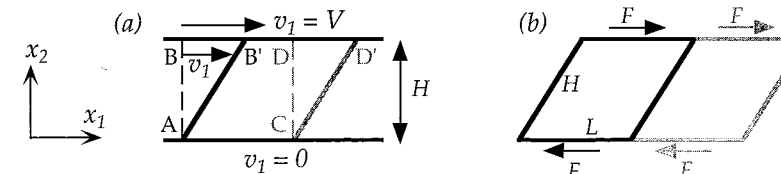


Figure 6.1. Shear flow in a layer of viscous fluid.

plate is stationary. Coordinates x_1 and x_2 are shown. If we could quickly inject a line of dye along the line AB, it would at a later time become inclined like the line AB'. Similarly the line CD will be carried into line CD'.

The box defined by ABDC becomes *deformed* into the parallelogram AB'D'C. This change in shape of the box is a measure of the deformation of the fluid. One way to measure the deformation of the box is with the ratio of lengths BB'/AB. If the time interval that has elapsed between when the dye is at AB and when it is at AB' is Δt , then we might write

$$\text{shape change} = V\Delta t/H$$

where H is the layer thickness. The *rate* of change of the shape or deformation is then measured by

$$\text{rate of deformation} = V/H$$

You can see that this quantity is a spatial gradient of velocity. In order to connect with the formal treatment in following sections, we will use the technical terminology. A quantity that measures deformation is called strain. Thus a quantity that measures rate of deformation is called a *strain rate*. Here I use the symbol s for strain rate. Also for consistency with later sections, I include a factor of one half in the definition of strain rate for Figure 6.1a:

$$s = \frac{V}{2H} \quad (6.1.1)$$

This quantity can serve as our measure of rate of deformation.

Now let us turn to the force causing the deformation. A force must be applied to the top plate in order to keep it moving. The moving plate then imparts a force into the adjacent fluid. The force F imparted into the top of the deformed box is depicted in Figure 6.1b as F . The magnitude of this force depends on the length, L , of the box. A second, adjacent box would also have a force F imparted into it, and the total force imparted into both boxes would be $2F$. However the deformation of each box is the same. Therefore what

counts is the *force per unit area* that is applied to the fluid. We are familiar with pressure being a force per unit area, but here I want to acknowledge that pressure is a special case of the more general concept of *stress*, so I will use that term here. We need to note at this point that Figure 6.1 is implicitly a cross-section through a structure that extends into the third dimension (out of the page). We can make this explicit by assuming that the box has a width W in the third dimension. Then the stress, τ , imparted to the top of the fluid is

$$\text{stress} = \frac{\text{force}}{\text{area}} = \tau = \frac{F}{LW} \quad (6.1.2)$$

This quantity will serve as our measure of the applied force causing deformation.

We can now define a viscous fluid as one in which strain rate is proportional to stress. To be consistent with the formal development to follow, I will again include a factor of two in the definition:

$$\tau = 2\mu s \quad (6.1.3)$$

The constant of proportionality, μ , is called the *viscosity*. Since strain rate has a dimension of 1/time and stress has dimensions of force/area, or pressure, the units of viscosity are pascal seconds or Pa s. (1 pascal = 1 newton/m²) A fluid with a high viscosity requires a greater stress to produce a given rate of deformation. Honey at room temperature has a viscosity in the range 10–100 Pa s. Water has a viscosity of about 0.001 Pa s. As we will see later, the mantle has a viscosity of the order of 10²¹ Pa s.

Equation (6.1.3) is a constitutive equation that describes the mechanical properties of a material. In order to use this in a study of convection, we need to draw upon some other basic principles: Newton's laws of motion, conservation of mass and conservation of energy. The latter will arise in Chapter 7. Here I will note how Newton's laws of motion and conservation of mass can be invoked for the situation in Figure 6.1.

The force F imparted by the top plate into the fluid induces a reaction of the fluid on the plate (Newton's first law, of action and reaction). The force will also be transmitted through the fluid to the bottom, where it will impart a force on the bottom plate, which in turn will induce an opposing reaction on the bottom of the fluid, shown as the lower force F . Newton's second law says that the acceleration of the fluid is proportional to the net force acting on it. Without saying so explicitly, I have been assuming so far that the

fluid is *not* accelerating, but is flowing with constant velocity. This requires that *the net force on the fluid is zero*. The forces acting on the fluid in the box in Figure 6.1b are the force F imparted from the top plate and the opposing reaction of the bottom plate to the motion of the fluid. I have shown these as having equal magnitude in anticipation of the requirement that they must sum to zero. Writing this out,

$$\text{Net force} = F + (-F) = 0 = \text{mass} \times \text{acceleration} = \text{mass} \times 0$$

This point deserves to be emphasised. I will state it a little more generally than I have illustrated so far:

In steady, slow viscous flow, all forces sum to zero everywhere in the fluid.

We are so used to thinking of forces producing accelerations that it is easy to overlook the implication of Newton's law in this context. In mantle convection, velocities are so small that accelerations are utterly negligible. In the slow viscous flow of the mantle, applied force is balanced by viscous resistance. Another way to say this is that *momentum is completely negligible in the mantle*. For example, the uplift produced by a plume rising through the mantle (Chapter 11) is caused not by the upward momentum of the plume material but by the buoyancy of the plume material. Sometimes the expression of Newton's second law is called the momentum equation, but here I will call it the force balance equation.

I will mention conservation of mass only briefly here. Two other unstated assumptions about Figure 6.1 are that the fluid velocity is independent of horizontal position, x_1 , and that the fluid is incompressible. It is then fairly obvious that the rate at which fluid flows into the box from the left is equal to the rate at which it flows out to the right. There is then no net accumulation of material and mass is conserved. If the fluid were compressible, then any imbalance of the flows into and out of the box would have to be balanced by a change in the density of the fluid in the box. For most purposes in this book we can treat the mantle as an incompressible fluid. The main context in which its compressibility is evident is in the increase of density with depth due to the great pressures in the interior (Chapter 5). However, the effect of this can be subtracted out of the equations of fluid motion to a good approximation. The equations for compressible fluids will be noted in passing in following sections.

To summarise this section, the mathematical description of flow in the mantle is done in terms of the concept of *strain rate*. The flow is driven by buoyancies, whose effect is represented as

stresses, and these stresses cause strains to change with time. The proportionality between stress and strain rate (for materials in which simple proportionality applies) is expressed as the *viscosity* of the fluid. For a viscous fluid undergoing very slow flow, accelerations are negligible, and driving forces are everywhere in balance with viscous resisting forces. For most purposes in this book, the mantle can be approximated as an incompressible fluid. The following four sections develop each of these aspects more generally.

6.2 Stress [Intermediate]

When forces act on the surface of a body, their effects are transmitted through the body. This means that if you picture an imaginary surface inside the body, the material on one side of the surface will exert a force on the material on the other side. The magnitude and direction of this force may depend on the orientation of the surface. For example, in Figure 6.2a, you can readily appreciate that there will be a normal force across the surface (i), but not across the surface (ii). Also the force may have any orientation relative to the surface across which it acts, that is it need not be normal to the surface: in a solid or a viscous fluid a tangential or shearing force component may also act. A *stress* is a force component *per unit area* acting across an arbitrarily oriented surface such as (iii) in Figure 6.2a. Stress thus has the same dimensions as pressure. Following engineering usage, I will denote stress as \mathbf{T} (for tension).

The full specification of a state of stress may require several stress components to be specified. For example, in Figure 6.2a we expect that there will be a normal stress across the surface (i) due to

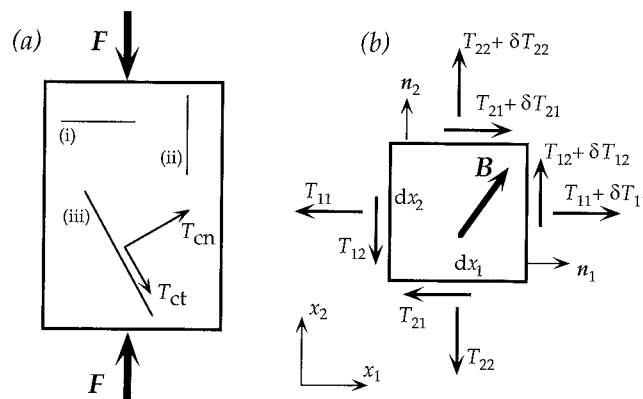


Figure 6.2. (a) Transmission of forces through a material. (b) Definitions of stress components.

the forces \mathbf{F} shown, and we should also specify that the normal stress is zero across the surface (ii), because no horizontal forces are applied. For the record, stress is a second-order tensor, but we need not worry unduly about what a tensor is: the relevant properties will become apparent in due course.

Stresses acting across the surface (iii) in Figure 6.2a are depicted as T_{cn} and T_{ct} . These two components are sufficient to specify any possible force acting across (iii), in two dimensions. The naming convention here is that each stress component is labelled with two subscripts, the first denoting the surface across which it acts, and the second denoting the direction of the stress component itself. Thus T_{cn} is a stress component acting across surface 'c' in the normal (n) direction, while T_{ct} acts across the same surface in the tangential direction. We will now use this in a more formal way.

A systematic way of specifying stresses is to refer their components to a coordinate system. This is done in Figure 6.2b, which has coordinates x_1 and x_2 . I will give the development, here and subsequently, in two dimensions where it is sufficient to demonstrate the concepts, since it is less messy than in three dimensions. The following can be generalised readily to three dimensions. Figure 6.2b depicts a small imaginary box inside a material, with faces oriented normal to the coordinate directions. Each face can be identified by its outward normal (n_1 and n_2). On each face stress components act, due to forces on the box exerted by surrounding material. For example, following the naming convention explained above, the component $(T_{11} + \delta T_{11})$ acts across the face whose normal n_1 is in the positive x_1 direction, and this component is also in the positive x_1 direction (I will explain the presence of the δT_{11} shortly).

The sign convention used here is that tensions are taken to be positive and compressions are taken to be negative. Further, stress components are positive when both they and the normal to the surface across which they act are in the positive coordinate direction. (Sometimes, particularly in the context of the earth's interior, pressure is taken to be positive, but this leads to confusion when shear stresses need to be considered, as we are about to do, so we will avoid this convention here.) If either the stress or the normal is in the negative coordinate direction, then the component is negative. If both are in the negative coordinate direction, then the component is positive.

The other component acting across the positive n_1 face is $(T_{12} + \delta T_{12})$ (in the direction of x_2). This is a positive shear stress component. On the left face, the component T_{11} is positive as shown, since it is in the negative x_1 direction across a face whose

normal is also in the negative x_1 direction. Similarly T_{12} on the left face is a positive component.

Another purpose of Figure 6.2b is to consider the force balance on the box in the situation where the stresses vary with position. Thus the normal stress on the right face, $(T_{11} + \delta T_{11})$, is different from the normal stress on the left face, T_{11} . If the box is not accelerating, then all the forces must balance. In two dimensions, there is the possibility of rotation, and so we must also consider torques or moments: these must also balance. Consider first the balance of torques about the centre of the box. First, the force exerted by the stress T_{12} is $(T_{12} \cdot dx_2)$, since stress is force per unit area, and the area over which T_{12} acts is dx_2 , assuming the box has unit length in the third dimension. Then the torque exerted about the centre is $(T_{12} \cdot dx_2)(dx_1/2)$. Considering each face in turn, the total torque in the clockwise direction is thus

$$(T_{21} + \delta T_{21}) \cdot dx_1 \cdot dx_2/2 - (T_{12} + \delta T_{12}) \cdot dx_2 \cdot dx_1/2 + T_{21} \cdot dx_1 \cdot dx_2/2 - T_{12} \cdot dx_2 \cdot dx_1/2 = 0 \quad (6.2.1)$$

Dividing by $dx_1 \cdot dx_2$ and taking the limit as the box size approaches zero, this yields

$$T_{12} = T_{21} \quad (6.2.2)$$

This is a fundamental property of the stress tensor: it is symmetric with respect to changes in the order of the indices.

Now consider the force balance in the x_1 direction. It will be useful as we do this to include a body force, depicted as \mathbf{B} in Figure 6.2b, which is a force per unit volume. \mathbf{B} will be a vector with components B_1 and B_2 . Then again considering each face in turn, and remembering that the tangential stresses on the top and bottom faces exert forces in the x_1 direction, the force balance condition is

$$(T_{11} + \delta T_{11}) \cdot dx_2 - T_{11} \cdot dx_2 + (T_{21} + \delta T_{21}) \cdot dx_1 - T_{21} \cdot dx_1 + B_1 \cdot dx_1 \cdot dx_2 = 0 \quad (6.2.3)$$

Dividing by $dx_1 \cdot dx_2$ and taking the limit, this yields

$$\frac{\partial T_{11}}{\partial x_1} + \frac{\partial T_{21}}{\partial x_2} + B_1 = 0 \quad (6.2.4a)$$

Similarly the force balance in the x_2 direction yields

$$\frac{\partial T_{12}}{\partial x_1} + \frac{\partial T_{22}}{\partial x_2} + B_2 = 0 \quad (6.2.4b)$$

In Box 6.B1 I introduce a notation that takes advantage of the repetitive forms of Equations (6.2.4) in order to reduce them to a more compact form. This is called the subscript notation with summation convention. Taking note of the symmetry of the stress tensor (Equation (6.2.2)), Equations (6.2.4a) and (6.2.4b) can be written concisely as

$$\frac{\partial T_{ij}}{\partial x_j} + B_i = 0 \quad (6.2.5)$$

This equation expresses the conservation of momentum, which in this context of no acceleration is equivalent to the equations of mechanical equilibrium or force balance. These equations show that the gradients of the stresses must obey these relationships if the material is to be in mechanical equilibrium. The presence of a body force modifies these relationships as shown. If the forms of these equations are unfamiliar, remember that they are simply the expression of the force balance in each coordinate direction.

Box 6.B1 Subscript notation and summation convention

The subscript notation permits concise expressions that would otherwise become large and clumsy, but it requires some familiarisation. I will briefly introduce it here, and provide some exercises at the end of the chapter.

You are probably familiar with subscripts being used to denote components of vectors and matrices. Thus a three-component vector can be written variously as

$$\mathbf{a} = \underline{a} = (a_1, a_2, a_3) = \{a_i\} \rightarrow a_i \quad (6.B1.1)$$

The form $\{a_i\}$ stands for the set of a_i , for all values of i . The last form is not strictly equivalent, since it stands for a_i , for *any* value of i . Thus a general component of \mathbf{a} stands for any component. This is the form we will use here.

The *summation convention* is that if a subscript is repeated in a term or product, it is implied that there is a summation over all values of that subscript. Thus the scalar product of two vectors can be written

$$\mathbf{a} \cdot \mathbf{b} = a_1 b_1 + a_2 b_2 + a_3 b_3 = \sum_{i=1}^3 a_i b_i = a_i b_i \quad (6.B1.2)$$

The last form employs the summation convention, since the subscript is repeated within the product. In effect the summation sign can be dropped because you know (usually) from the context which values the subscript can take. Occasionally there are situations where this is not true, and the explicit summation must be shown.

Summations are implicit in the following examples.

$$a_{ii} = a_{11} + a_{22} + a_{33} \quad (6.B1.3)$$

$$a_{ij}b_j = a_{i1}b_1 + a_{i2}b_2 + a_{i3}b_3 \quad (6.B1.4)$$

$$\frac{\partial a_i}{\partial x_i} = \frac{\partial a_1}{\partial x_1} + \frac{\partial a_2}{\partial x_2} + \frac{\partial a_3}{\partial x_3} = \nabla \cdot \mathbf{a} \quad (6.B1.5)$$

However there is no implied summation in

$$a_i + b_i \quad (6.B1.6)$$

which stands simply for the sum of any corresponding pair of components of \mathbf{a} and \mathbf{b} , such as $a_2 + b_2$. This is because the index is not repeated *within* a term or product. Sometimes you need to turn the summation convention off. Thus if you want to refer to *any* diagonal component of a_{ij} , you must say explicitly ‘ a_{ii} (no summation)’.

A repeated index is, in effect, an internal dummy index that does not appear in the total expression. Thus, in Equation (6.B1.4), the end result is a vector component with index i , the j having been summed out. This means also that the name of the summed index is internal. Thus it is quite valid to write

$$a_{ii} = a_{kk} \quad (6.B1.7)$$

Correspondingly, a summation reduces the *order* of the term, that is the number of unsummed subscripts. Thus, in Equation (6.B1.3), \mathbf{a} is a second-order tensor, but a_{ii} is a scalar (a zero-order tensor).

Just as a scalar cannot be added to a vector, all terms in an expression must be of the same order. Thus

$$a_i b_i + c_i$$

is not valid, but

$$a_i b_i + d$$

is valid.

The role of the Kronecker delta is worth spelling out. It is defined as

$$\delta_{ij} = 1 \text{ if } i = j$$

$$\delta_{ij} = 0 \text{ if } i \neq j \quad (6.B1.8)$$

and is analogous to a unit matrix $\mathbf{I} = [\delta_{ij}]$. When it occurs in a sum, its effect is to select out one term from the sum. Thus

$$a_i \delta_{i2} = a_1 \delta_{12} + a_2 \delta_{22} + a_3 \delta_{32} = 0 + a_2 + 0 = a_2 \quad (6.B1.9)$$

and

$$b_{ijk} \delta_{km} = b_{ijm} \quad (6.B1.10)$$

6.2.1 Hydrostatic pressure and deviatoric stress

In the special case where the state of stress is a hydrostatic pressure, the normal components, like T_{11} , are all equal and the tangential components are zero. Thus, in three dimensions,

$$\begin{aligned} T_{11} &= T_{22} = T_{33} = -P \\ T_{12} &= T_{13} = T_{23} = 0 \end{aligned} \quad (6.2.6a)$$

where I have taken pressure to be positive in compression, whereas T is positive in tension. Another way to write this, using the subscript notation and the Kronecker delta (Box 6.B1), is

$$T_{ij} = -P \delta_{ij} \quad (6.2.6b)$$

The use of this sign convention for T may seem inappropriate for the earth’s interior, where the state of stress is one of minor deviations from overwhelming pressure, but the equations are simpler with this convention. As well, for most of our purposes here, the large hydrostatic pressure can be subtracted out. This is because flow is not driven by hydrostatic pressure, but depends on deviations from hydrostatic pressure. This motivates the idea of *deviatoric stress*, below.

First, we can generalise the idea of pressure by defining P in a general state of stress (that is, other than that defined in Equations (6.2.6)) as

$$P = -(T_{11} + T_{22} + T_{33})/3 = -T_{ii}/3 \quad (6.2.7)$$

In other words, pressure is defined as the negative of the average of the normal stress components.

We can now define a *deviatoric stress*, τ_{ij} , as the total stress minus the average of the normal stress components, so that

$$\tau_{ij} = T_{ij} - T_{kk} \delta_{ij}/3 = T_{ij} + P \delta_{ij} \quad (6.2.8)$$

The pressure term in the last form is positive because of the different sign conventions of pressure and stress. A different subscript, k ,

is used in the summation in the first form so there is no confusion with the subscripts i and j , which can take arbitrary values in this equation. The effect of the Kronecker delta is that only the diagonal components of the stress are modified. In explicit matrix form, τ_{ij} is equivalent to

$$\tau_{ij} \Rightarrow \begin{bmatrix} T_{11} + P & T_{12} & T_{13} \\ T_{21} & T_{22} + P & T_{23} \\ T_{31} & T_{32} & T_{33} + P \end{bmatrix}$$

The deviatoric stress is that part of a general state of stress that differs from hydrostatic pressure or isotropic stress, and it is the part that can generate fluid flow.

6.3 Strain [Intermediate]

Strain is a measure of deformation. There are in fact many different measures that might be used to characterise deformation, and it is a matter of convenience which one is chosen. We will make choices here that are convenient for the present purpose. When deformation occurs, different parts of a body are displaced by different amounts. In other words there are spatial gradients of displacement. Displacement relates two different positions of a body. For example, Figures 6.3a and 6.3b depict a body in different positions at different times. Suppose the initial position of a point in the body is x_i^0 and the final position is x_i . Then the displacement of the point is defined as

$$u_i = x_i - x_i^0 \quad (6.3.1)$$

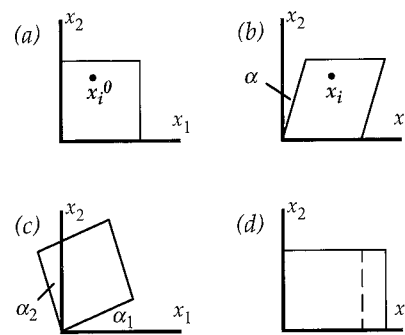


Figure 6.3. Definitions of displacement and strain.

Different parts of the body in Figure 6.3b are displaced by different amounts relative to their initial position. The variation of the two components of displacement with position is described by

$$u_1 = bx_2, \quad u_2 = 0$$

where b is a constant. In other words the displacement in the x_1 direction increases with increasing x_2 , and there are no displacements in the x_2 direction. Thus there is a gradient of displacement u_1 :

$$\frac{\partial u_1}{\partial x_2} = b = -\tan \alpha$$

where α is the (counter-clockwise) angle through which the body has been sheared in this deformation. In Section 6.1 we used a displacement gradient like this to characterise the deformation of the fluid layer, and we can use the same idea here, as we will see.

If there is a shearing in the other orientation as well, parallel to x_2 as illustrated in Figure 6.3c, then

$$\tan \alpha_1 = \frac{\partial u_2}{\partial x_1}$$

$$\tan \alpha_2 = -\frac{\partial u_1}{\partial x_2}$$

taking counter-clockwise rotations to be positive.

Now if $\alpha_1 = \alpha_2$, then the body has simply rotated with no deformation. Since rotation does not involve any internal deformation of the body, we need a way to distinguish deformation from solid-body rotation. For example, $(\alpha_1 - \alpha_2)$ is zero if there is only rotation and no deformation ($\alpha_1 = \alpha_2$), and non-zero if there is deformation, so it can serve as a measure of deformation. On the other hand, if $\alpha_2 = -\alpha_1$ then there is no net rotation, in which case $(\alpha_1 + \alpha_2)$ is zero and the body undergoes pure shear. If $(\alpha_1 + \alpha_2)$ is non-zero there is rotation, so $(\alpha_1 + \alpha_2)$ can serve as a measure of rotation. These ideas are used to define a strain tensor and a rotation tensor. However, instead of the angles of rotation, we will use their tangents, which are the displacement gradients noted above. In the example of Figure 6.3c, a measure of rotation is

$$\omega_{12} = \frac{1}{2}(\tan \alpha_1 + \tan \alpha_2) = \frac{1}{2}\left(\frac{\partial u_2}{\partial x_1} - \frac{\partial u_1}{\partial x_2}\right) \quad (6.3.2)$$

and a measure of deformation is

$$e_{12} = \frac{1}{2}(\tan \alpha_1 - \tan \alpha_2) = \frac{1}{2}\left(\frac{\partial u_1}{\partial x_2} + \frac{\partial u_2}{\partial x_1}\right) \quad (6.3.3)$$

Now let us look at a different kind of deformation. Figure 6.3d depicts a stretching deformation (relative to Figure 6.3a). It is described by

$$u_1 = cx_1, \quad u_2 = 0$$

where c is a constant, and the associated displacement gradient is $\partial u_1 / \partial x_1 = c$. In this case there is no rotation to worry about, so the displacement gradient will serve as it stands as a measure of this deformation:

$$e_{11} = \frac{\partial u_1}{\partial x_1} \quad (6.3.4)$$

Using the gradient of the displacement in this case distinguishes deformation from simple solid-body translation: in a simple translation to the right, u_1 is constant, so $c = 0$ and $e_{11} = 0$.

We can now collect these ideas together concisely by defining a *strain tensor*

$$e_{ij} = \frac{1}{2}\left(\frac{\partial u_i}{\partial x_j} + \frac{\partial u_j}{\partial x_i}\right) \quad (6.3.5)$$

and an *infinitesimal rotation tensor*

$$\omega_{ij} = \frac{1}{2}\left(\frac{\partial u_j}{\partial x_i} - \frac{\partial u_i}{\partial x_j}\right) \quad (6.3.6)$$

The latter is called infinitesimal because strictly it measures angles of rotation only for small angles.

It is obvious from the definition that e_{ij} is symmetric. You can easily see that the definition of e_{ij} includes the case of Equation (6.3.3). In the case of the stretching deformation of Figure 6.3d, it yields

$$e_{11} = \frac{1}{2}\left(\frac{\partial u_1}{\partial x_1} + \frac{\partial u_1}{\partial x_1}\right) = \frac{\partial u_1}{\partial x_1}$$

so it serves for this case too. Examples of other kinds of deformation and the strains that measure them are given as exercises at the

end of the chapter, and I recommend that you work through these to gain some familiarity with how this strain tensor works. We will not be concerned much further with rotation.

There is one special case of deformation worth spelling out, namely a change of volume. If there is stretching in each of three dimensions, then a small cube would expand, and its new volume would be

$$V = V_0(1 + e_{11})(1 + e_{22})(1 + e_{33}) \approx V_0(1 + e_{11} + e_{22} + e_{33})$$

The relative change in volume is then

$$\begin{aligned} (V - V_0)/V_0 &= e_{11} + e_{22} + e_{33} \\ &= e_{ii} = \partial u_i / \partial x_i = \nabla \cdot \mathbf{u} \equiv \Theta \end{aligned} \quad (6.3.7)$$

This quantity Θ is called the *dilatation*, and it is just the divergence of \mathbf{u} .

By analogy with the definition of deviatoric stress, we can define a *deviatoric strain*. Instead of subtracting out an average isotropic stress (that is, a pressure), we subtract out an average isotropic strain, that is, a dilatation. In this case our sign convention for dilatation is the same as for general strains, so we get

$$\xi_{ij} = e_{ij} - \Theta \delta_{ij}/3 = e_{ij} - e_{kk} \delta_{ij}/3 \quad (6.3.8)$$

You can see the analogy with Equation (6.2.8). This has the property that its diagonal terms sum to zero:

$$\xi_{ii} = e_{ii} - e_{kk} = 0$$

Thus ξ_{ii} does not register a change in volume, only a change in shape. It will be useful in discussing the viscosity of fluids in Section 6.5.

6.4 Strain rate [Intermediate]

It is easy to extend the definition of strain to its rate of change with time. In this case, the rate of displacement of a point in a body is just its velocity, \mathbf{v} , so differentiation of Equation (6.3.5) with respect to time yields

$$s_{ij} \equiv \frac{\partial e_{ij}}{\partial t} = \frac{1}{2}\left(\frac{\partial v_i}{\partial x_j} + \frac{\partial v_j}{\partial x_i}\right) \quad (6.4.1)$$

and s_{ij} is a *strain rate* tensor. This is analogous to Equation (6.1.1), in which we used a velocity gradient to measure the rate of shear of the fluid layer in Section 6.1. The *rate of dilatation* is the divergence of the velocity:

$$\frac{\partial \Theta}{\partial t} = s_{kk} = \frac{\partial v_k}{\partial x_k} = \nabla \cdot \mathbf{v}$$

and a *deviatoric strain rate* tensor is

$$\zeta_{ij} = s_{ij} - s_{kk}\delta_{ij}/3 \quad (6.4.2)$$

A good way to think of this quantity is that, with volume changes removed, it measures the rates of shearing deformations, or rates of changes of shape at constant volume.

6.5 Viscosity [Intermediate]

A viscous fluid is one that resists shearing deformations. Strictly speaking, it is one for which there is a linear relationship between strain rate and stress. Such fluids are sometimes called Newtonian or linear viscous fluids. You will see in Section 6.10 that more general relationships occur. The fluids of common experience are viscous, though for air and water the viscosity is quite low. Honey and treacle (molasses) are more viscous, especially when cold.

The simplest explication of viscosity is in a situation where the fluid is undergoing simple shear, as was depicted in Figure 6.1. The top plate is moving to the right, the bottom plate is stationary, and the line AB is displaced into the line AB' . The only non-zero velocity gradient is $\partial v_1 / \partial x_2$, and the non-zero strain rate components are, using the definition Equation (6.4.1)

$$s_{12} = s_{21} = \frac{1}{2} \frac{\partial v_1}{\partial x_2}$$

In a linear viscous fluid, the non-zero deviatoric stress components would then be

$$\tau_{12} = \tau_{21} = \mu \frac{\partial v_1}{\partial x_2} = 2\mu s_{12} \quad (6.5.1)$$

where the constant of proportionality is μ , the *viscosity*. This is equivalent to Equation (6.1.3) derived earlier.

The viscosity μ is defined here following the convention used by Batchelor [2] in which it is the ratio of the stress component to

the velocity gradient, which leaves a factor of 2 in the ratio of stress to strain rate. Sometimes a viscosity is defined by the ratio of stress to strain rate; for this I will use the symbol η . It differs from μ by a factor of 2:

$$\tau_{12} = \eta s_{12}, \quad \eta = 2\mu \quad (6.5.2)$$

The definition of viscosity in cases with more general stresses and strains than the simple shearing depicted in Figure 6.1 requires some care at this point. It is usually assumed that fluids exhibit viscous behaviour only with respect to shearing deformations. Shearing deformations are measured by the deviatoric strain rate defined by Equation (6.4.2). It is conceivable that a fluid might also exhibit a viscous resistance to volume changes (in addition to its elastic resistance to compression). That is to say, the resistance to compression might depend on the *rate of compression* (viscous resistance), as well as on the degree of compression (elastic resistance). We could then define a *bulk viscosity*, by analogy with the bulk modulus of elasticity. However, I follow the usual practice of assuming that the bulk viscosity is negligible. The purpose of this digression has been to motivate the particular general form of the relationship between stress and strain rate that I am about to present.

If we simply generalise Equation (6.5.1) to all components, $\tau_{ij} = 2\mu s_{ij}$, there are two potential problems. First, it would imply that a bulk viscosity exists. Second, it would imply that the bulk viscosity is the same as the shear viscosity, and this is not necessarily so (the molecular mechanisms resisting deformation, if any, might well be different in compression from those that operate in shear). To avoid these problems, we can define viscous behaviour to apply only between *deviatoric stress* and *deviatoric strain rate*. Then neither pressure nor volume changes appear in the relationship. Thus

$$\begin{aligned} \tau_{ij} &= 2\mu \zeta_{ij} \\ &= 2\mu(s_{ij} - s_{kk}\delta_{ij}/3) \end{aligned} \quad (6.5.3)$$

This is a general constitutive relationship for a *compressible linear viscous fluid*.

Sometimes the compressibility of a fluid is negligible, and it can be treated as incompressible. In this case $\partial \Theta / \partial t = s_{kk} = 0$, and Equation (6.5.3) simplifies to

$$\tau_{ij} = 2\mu s_{ij} \quad [\text{incompressible}] \quad (6.5.4)$$

Although the earth's mantle material is compressed about 30% by volume near its base, the effect of compression can be subtracted out, to a sufficient approximation for many purposes (Chapter 7). The mantle can then be treated as incompressible, and Equation (6.5.4) can be used.

6.6 Equations governing viscous fluid flow [Intermediate]

In order to quantify the dynamics of viscous fluid flow, we must combine the constitutive relation of the fluid with equations expressing conservation of mass, momentum and energy. As we discussed in Section 6.1, acceleration and inertia are negligible in the mantle, so conservation of momentum reduces to a force balance. In the context of mantle convection, conservation of energy involves heat, which will be considered in Chapter 7.

6.6.1 Conservation of mass

For most purposes in this book, we can assume that the mantle is an incompressible fluid. For this case, conservation of mass becomes conservation of fluid volume. Then the rate at which fluid flows into a small volume like that depicted in Figure 6.4 must equal the rate at which it flows out. The volume of fluid that flows through the left side of the box in a time interval dt is equal to $v_1 \cdot dt \cdot dx_2$. The contributions through all four sides should sum to zero:

$$[v_1 dx_2 + v_2 dx_1 - (v_1 + dv_1)dx_2 - (v_2 + dv_2)dx_1]dt = 0$$

Dividing this by $dt \cdot dx_1 \cdot dx_2$ yields

$$\frac{\partial v_1}{\partial x_1} + \frac{\partial v_2}{\partial x_2} = \frac{\partial v_i}{\partial x_i} = \nabla \cdot \mathbf{v} = 0 \quad [\text{incompressible}] \quad (6.6.1)$$

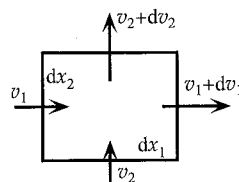


Figure 6.4. Flows into and out of a small region, used to derive the equation for conservation of mass.

$$\frac{\partial \rho}{\partial t} + v_i \frac{\partial \rho}{\partial x_i} + \rho \frac{\partial v_i}{\partial x_i} = 0 \quad (6.6.2)$$

In vector notation, the middle term is $\mathbf{v} \cdot \nabla \rho$.

6.6.2 Force balance

We have seen already in Section 6.2 that the general condition for stress components and body forces to be balanced, so that fluid elements do not undergo acceleration, is expressed by Equation (6.2.5). The deviatoric stresses arising from the flow of a viscous fluid are expressed by Equation (6.5.3) or (6.5.4), and the deviatoric stresses are related to total stress through Equation (6.2.8). We can now combine these into a more specific equation. Here I just follow the incompressible case. The total stress is (Equations (6.2.8), (6.5.4))

$$\begin{aligned} T_{ij} &= \tau_{ij} - P\delta_{ij} \\ &= 2\mu s_{ij} - P\delta_{ij} \end{aligned}$$

and the general force balance for an *incompressible* viscous fluid is then (Equation (6.2.5))

$$2 \frac{\partial(\mu s_{ij})}{\partial x_j} - \frac{\partial P}{\partial x_i} + B_i = 0 \quad (6.6.3)$$

This equation simplifies if the viscosity is independent of position. The assumption of constant viscosity is common outside of the mantle flow context, and it is useful for some purposes in this book, so I note some special forms of the equations for this case as we go along. If μ is independent of position, then Equation (6.6.3) becomes

$$2\mu \frac{\partial s_{ij}}{\partial x_j} - \frac{\partial P}{\partial x_i} + B_i = 0$$

This can be put in terms of velocity gradients using the definition (6.4.1) of s_{ij} . First, you can see that

$$\begin{aligned} 2 \frac{\partial s_{ij}}{\partial x_j} &= \frac{\partial}{\partial x_j} \left(\frac{\partial v_i}{\partial x_j} + \frac{\partial v_j}{\partial x_i} \right) = \frac{\partial^2 v_i}{\partial x_j \partial x_j} + \frac{\partial}{\partial x_i} \left(\frac{\partial v_j}{\partial x_j} \right) \\ &= \frac{\partial^2 v_i}{\partial x_j \partial x_j} \\ &= \nabla^2 v_i \end{aligned}$$

where the second line follows from the continuity equation (6.6.1), which says that $(\partial v_j / \partial x_j) = 0$ for an incompressible fluid. The third line defines what is called the *Laplacian operator*:

$$\begin{aligned}\nabla^2 &= \nabla \cdot \nabla = \frac{\partial}{\partial x_k} \frac{\partial}{\partial x_k} \\ &= \frac{\partial^2}{\partial x_1^2} + \frac{\partial^2}{\partial x_2^2} + \frac{\partial^2}{\partial x_3^2}\end{aligned}\quad (6.6.4)$$

The denominator term $(\partial x_k \partial x_k)$ is written in this repeating form so that the summation convention is seen explicitly to apply. The term ∂x_k^2 would be ambiguous in this respect.

Now, finally, the force balance equation for an *incompressible, constant-viscosity* viscous fluid becomes

$$\mu \nabla^2 v_i - \frac{\partial P}{\partial x_i} + B_i = 0 \quad (6.6.5a)$$

or

$$\mu \frac{\partial^2 v_i}{\partial x_j \partial x_j} - \frac{\partial P}{\partial x_i} + B_i = 0 \quad (6.6.5b)$$

6.6.3 Stream function (incompressible, two-dimensional flow)

A further simplification of the equations is possible when the fluid is incompressible and the flow is two-dimensional, that is to say when one velocity vector component is zero. It is then possible to define a function that allows the continuity and force balance equations to be put into other mathematically useful forms. In this case, the continuity equation (6.6.1) is

$$\frac{\partial v_1}{\partial x_1} + \frac{\partial v_2}{\partial x_2} = 0 \quad (6.6.6)$$

If we define a *stream function* ψ such that

$$v_1 = \frac{\partial \psi}{\partial x_2}, \quad v_2 = -\frac{\partial \psi}{\partial x_1} \quad (6.6.7)$$

then you can see by substitution that the continuity equation is satisfied identically.

In two dimensions, the horizontal and vertical force balance equations for an incompressible, constant viscosity fluid are (Equation (6.6.5a))

$$\begin{aligned}\mu \nabla^2 v_1 - \frac{\partial P}{\partial x_1} + B_1 &= 0 \\ \mu \nabla^2 v_2 - \frac{\partial P}{\partial x_2} + B_2 &= 0\end{aligned}$$

If the horizontal equation is differentiated with respect to x_2 , the vertical equation differentiated with respect to x_1 , and the second subtracted from the first, the result is

$$\mu \nabla^2 \left(\frac{\partial v_1}{\partial x_2} - \frac{\partial v_2}{\partial x_1} \right) + \left(\frac{\partial B_1}{\partial x_2} - \frac{\partial B_2}{\partial x_1} \right) = 0$$

and the pressure terms have cancelled out. Substitution from the definition (6.6.7) of ψ then yields

$$\mu \nabla^2 (\nabla^2 \psi) + \left(\frac{\partial B_1}{\partial x_2} - \frac{\partial B_2}{\partial x_1} \right) = 0 \quad (6.6.8)$$

If there are no body forces

$$\nabla^4 \psi = 0 \quad (6.6.9)$$

where $\nabla^4 = \nabla^2 \nabla^2$ is called the *biharmonic operator*, and Equation (6.6.9) is called the *biharmonic equation*.

Equations (6.6.8) and (6.6.9) ensure that both the continuity equation and the force balance equations are satisfied. Thus the stream function allows the flow equations to be expressed in a very compact form. You will see below that it also leads to some useful analytic solutions to the flow equations.

The usefulness of the stream function does not stop there. Its name derives from the fact that lines of constant ψ are lines along which fluid flows. To see this, consider the difference, $d\psi$, between two close points, P and Q, depicted in Figure 6.5a:

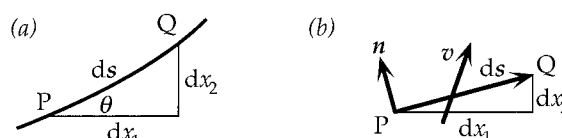


Figure 6.5. Geometric relationships to elucidate stream functions.

$$\begin{aligned} d\psi &= \frac{\partial \psi}{\partial x_1} dx_1 + \frac{\partial \psi}{\partial x_2} dx_2 \\ &= -v_2 dx_1 + v_1 dx_2 \\ &= -v_2 ds \cos \theta + v_1 ds \sin \theta \end{aligned}$$

Now if the line element \mathbf{ds} is chosen to be parallel to the velocity \mathbf{v} , then

$$v_1 = v \cos \theta, \quad v_2 = v \sin \theta$$

which implies, upon substitution, that $d\psi = 0$. In this case, ψ would have the same value at P and Q. It follows that if \mathbf{ds} is part of a curve that is parallel to the local velocity along its length, then ψ is a constant along this curve.

Another property of the stream function is that the velocity is proportional to the local gradient of the stream function. This means that if streamlines are defined at equal intervals of ψ , like topographic contours, the velocity is inversely proportional to their spacing. This property can be shown using Figure 6.5b. The volumetric rate of flow dV through the surface defined by the line \mathbf{ds} joining P and Q and extending a unit distance in the third dimension (out of the page) is $\mathbf{v} \cdot \mathbf{n} ds$ where \mathbf{n} is the unit normal to the surface. The vector \mathbf{n} has components

$$\mathbf{n} = (-dx_2, dx_1)/ds$$

Thus the flow rate is

$$dV = -v_1 dx_2 + v_2 dx_1 = -d\psi$$

the latter step being from the definition (6.6.7) of ψ . The volume flux ϕ is the volume flow rate per unit area:

$$\phi = dV/ds = -d\psi/ds$$

and if \mathbf{ds} is chosen to be oriented normal to the local velocity, this is just the vector gradient of ψ .

6.6.4 Stream function and force balance in cylindrical coordinates [Advanced]

It will be useful for considering mantle plumes later to have the flow equations in a form convenient for solving problems with axial symmetry. Since my focus here is on presenting the central physical

arguments in the most direct possible way, rather than on mathematical elaborations, I give only an abbreviated development here, fuller treatments being available elsewhere [2, 3].

The stream function defined by Equations (6.6.7) can be viewed as one component of a vector potential $(0, 0, \psi)$. The Cartesian velocities are then given by $\mathbf{v} = \nabla \times (0, 0, \psi)$. An analogous form can be used when there is axial symmetry. However with axial symmetry there are two possibilities. The first is to carry the so-called *Lagrangian* stream function ψ directly over. This preserves the relationship between velocity and derivative of the stream function. The second is to include a factor of $1/r$ to preserve the relationship between the stream function and the volume flux, which is proportional to (rv) . The latter approach yields the *Stokes* stream function, Ψ , defined such that

$$\mathbf{v} = -\nabla \times \left(\frac{\Psi}{r} \mathbf{i}_\varphi \right) \quad (6.6.10)$$

where \mathbf{i}_φ is a unit vector in the cylindrical coordinate system (r, φ, z) depicted in Figure 6.6.

The velocity components are

$$v_r = \frac{1}{r} \frac{\partial \Psi}{\partial z}, \quad v_z = -\frac{1}{r} \frac{\partial \Psi}{\partial r} \quad (6.6.11)$$

To express the force balance equation in cylindrical coordinates, it is useful to define a *vorticity*

$$\boldsymbol{\Omega} = \nabla \times \mathbf{v} \quad (6.6.12)$$

With axial symmetry there is only one non-zero component: $\boldsymbol{\Omega} = (0, \Omega, 0)$. Ω is twice the rate of change of the rotation tensor ω_{12} defined by Equation (6.3.2); the factor of 2 is for convenience here and is often omitted from the definition. Substitution of the

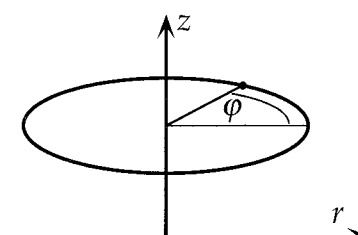


Figure 6.6. Cylindrical coordinates for axially symmetric problems.

velocity components of Equation (6.6.11) into this definition yields, after some manipulation

$$\Omega = \frac{1}{r} E^2 \Psi \quad (6.6.13)$$

where E^2 is a differential operator related to the Laplacian operator ∇^2 of Equation (6.6.4):

$$\begin{aligned} E^2 &= r \frac{\partial}{\partial r} \left(\frac{1}{r} \right) \frac{\partial}{\partial r} + \frac{\partial^2}{\partial z^2} \\ &= \nabla^2 - \frac{2}{r} \frac{\partial}{\partial r} \end{aligned} \quad (6.6.14)$$

For the incompressible fluid being considered here, vector identities yield

$$\nabla \times \boldsymbol{\Omega} = -\nabla^2 \mathbf{v}$$

Then the force balance equation (6.6.5a), with no body forces, can be written

$$\mu \nabla \times \boldsymbol{\Omega} = -\nabla P$$

and taking the curl yields

$$\nabla^2 \boldsymbol{\Omega} = i_\varphi \left(\nabla^2 \Omega - \frac{\Omega}{r^2} \right) = 0 \quad (6.6.15)$$

and

$$E^2 \Omega + \frac{2}{r} \frac{\partial \Omega}{\partial r} - \frac{\Omega}{r^2} = 0$$

Finally this can be manipulated into the form

$$E^4 \Psi = E^2 E^2 \Psi = 0 \quad (6.6.16)$$

The analogy with Equation (6.6.9) for the Cartesian case is evident. Again we have the continuity and force balance equations put into a compact form that will be used in Section 6.8.

6.7 Some simple viscous flow solutions

Some flow solutions in relatively simple situations will help you to gain more physical insight into how viscous flow works. Additional exercises are provided at the end of the chapter.

6.7.1 Flow between plates

In the situation depicted earlier in Figure 6.1, flow is driven by the top moving plate. There are no body forces and there is no pressure gradient. In this situation the force balance Equation (6.6.5b) becomes

$$\frac{\partial^2 v_1}{\partial x_2^2} = 0$$

With the boundary conditions depicted, the solution to this is $v_1 = Vx_2/H$. This solution actually justifies the assumption implicit in Figure 6.1 that the velocity variation across the layer is linear.

Suppose now that both plates are stationary but there is a horizontal pressure gradient specified by

$$P = P_0 - P' x_1$$

as depicted in Figure 6.7. Then Equation (6.6.5b) becomes

$$\frac{\partial^2 v_1}{\partial x_2^2} = -\frac{P'}{\mu} \quad (6.7.1)$$

with the solution

$$v_1 = \frac{P'}{2\mu} (H - x_2)x_2 \quad (6.7.2)$$

Thus the velocity profile is parabolic, with a maximum at the centre of the layer. It will be useful for later to calculate the volumetric flow rate, Q , through this layer:

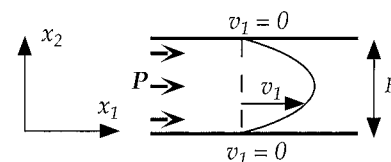


Figure 6.7. Flow between plates driven by a pressure gradient.

$$Q = \int_0^H v_1 dx_2 = \frac{P' H^3}{12\mu} \quad (6.7.3)$$

Thus Q is proportional to the cube of the layer thickness.

This solution illustrates the fundamental point made earlier about slow viscous flow, that the flow is determined by a local balance between a driving pressure gradient and viscous resistance.

6.7.2 Flow down a pipe

It will be useful for later to derive the analogous flow through a pipe. I will present this problem from first principles rather than starting from the rather mathematical approach of the cylindrical stream function equation of Section 6.6.4. This will reveal even more directly the local balance between the driving force and the viscous resistance.

Here I assume that the pipe is vertical and the flow is driven by the weight of the fluid, rather than by a pressure gradient. This situation is directly analogous to convection, in which there is a balance between buoyancy forces and viscous resistance. It will have particular application in the theory of mantle plumes of Chapter 11.

Figure 6.8 depicts a fluid of density ρ flowing down a pipe (radius a) under the action of its own weight. A fluid element of length dz and radius r , like that shown, has weight

$$W(r) = \pi r^2 \cdot dz \cdot \rho g$$

This is balanced by viscous resistance R acting on the sides of the element. If the flow is steady, there will be no net force on the top and bottom of the element. The viscous stress will be proportional to the local radial gradient of the vertical velocity: $\mu \cdot \partial v / \partial r$. The total resisting force is this stress times the surface area, $2\pi r \cdot dz$, over which it acts. Thus

$$R(r) = 2\pi r \cdot dz \cdot \mu \cdot \partial v / \partial r$$

A balance of forces requires $R + W = 0$, which yields

$$\frac{\partial v}{\partial r} = -\frac{\rho g}{2\mu} r$$

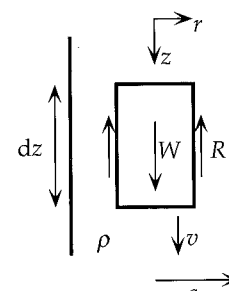


Figure 6.8. Force balance and viscous flow down a pipe.

Comparison with Equation (6.7.1) shows that the weight of the fluid here is playing the same role, through the term (ρg) , as the pressure gradient in the plate problem of Figure 6.7.

The solution for this problem in which the fluid velocity is zero at the walls of the pipe is

$$v = \frac{\rho g}{4\mu} (a^2 - r^2) \quad (6.7.4)$$

and the volumetric flow rate is

$$Q = \frac{\pi \rho g}{8\mu} a^4 \quad (6.7.5)$$

The velocity profile is parabolic, as in the plate problem, but Q depends on a higher power of the size of the conduit than in the planar case, since the fluid is resisted all around in the pipe, but only from the top and bottom between the plates.

6.8 Rise of a buoyant sphere

A blob of buoyant fluid rising slowly through a viscous fluid, with negligible momentum, adopts the shape of a sphere. Drops and bubbles are commonly approximately spherical in shape, but in common situations the reason is mainly because of surface tension. The effect of momentum is also involved with water drops and bubbles of air in water, which usually causes distortions. One can observe some cases where drops and bubbles are more nearly spherical, such as air bubbles in honey, or the buoyant blobs in a 'lava lamp'. The mathematical analysis by Batchelor [2] shows more rigorously that the preferred shape is spherical.

The rise of a buoyant sphere is relevant to the mantle because there is good reason to believe that a new plume begins as a large spherical 'head', as we will see in Chapter 11. It is instructive to consider this case because it is relatively simple in concept, and because again it illustrates the balance between buoyancy and viscous resistance. It also is an appropriate example to demonstrate the usefulness of rough estimates. Not only can these give reasonable numerical estimates, but they reveal the scaling properties in the problem, by which I mean the way the behaviour would change if parameters or material properties were different.

6.8.1 Simple dimensional estimate

Let me begin by posing the question of how long it would take a plume head to rise through the mantle. In the absence of any prior indication, we might not know whether it would take ten thousand years or a billion years. Almost any kind of rough estimate would improve on this level of our ignorance. To obtain an initial estimate, consider the sphere sketched in Figure 6.9. *Buoyancy*, technically, is the *total force* arising from the action of gravity on the density difference between the sphere and its surroundings. Thus the buoyancy of the sphere is

$$B = -4\pi r^3 g \Delta\rho / 3 \quad (6.8.1)$$

This force will cause the sphere to rise if the density of the sphere is less than that of its surroundings, so that $\Delta\rho$ is negative. The velocity, v , at which the sphere rises will be such that the viscous resistance from the surrounding material balances this buoyancy force. This velocity is measured relative to fluid at a large distance.

We can estimate the viscous resistance as follows. Viscous stress is proportional to strain rate, as described in Sections 6.1 and 6.5. Strain rate is proportional to velocity gradients. If we assume that the upward flow velocity in the fluid is about v near the sphere and decreases to a fraction of v over a distance of one sphere radius, then the velocity gradient will be of the order of v/r . More importantly, if v or r is changed, the velocity gradients will change in proportion. Thus, even without knowing the details of the flow and of the velocity gradients, by taking the strain rate to be of the order of v/r we can incorporate the idea that it will be ten times larger if v is ten times larger or if r is ten times *less*.

Now viscous stress, τ , is viscosity times strain rate, so

$$\tau = c\mu v/r$$

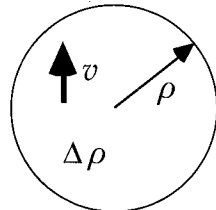


Figure 6.9. A buoyant sphere of density contrast $\Delta\rho$ rising with velocity v .

$$R = -4\pi r^2 \cdot c\mu v/r = -4\pi c r \mu v \quad (6.8.2)$$

where the minus sign comes from taking upwards to be positive. The forces on the sphere will be balanced, and hence its velocity

will be constant, if $B + R = 0$. So, using Equations (6.8.1) and (6.8.2),

$$4\pi c r \mu v + 4\pi r^3 g \Delta\rho / 3 = 0$$

The value of the steady velocity will thus be

$$v = -g \Delta\rho r^2 / 3c\mu \quad (6.8.3)$$

If v is less than this value, the resistance will be less than the buoyancy, and the sphere will accelerate. If v is greater, the sphere will decelerate. Thus this value of v is a stable equilibrium value to which v will tend after any perturbation of the sphere's motion.

A more rigorous theory for a solid sphere is presented below. A solution for a fluid sphere with a viscosity, μ_s , different from the surrounding fluid can be obtained by a similar approach. These theories confirm the form of Equation (6.8.3), and yield

$$c = \frac{\mu + 1.5\mu_s}{\mu + \mu_s} \quad (6.8.4)$$

The value of c ranges between 1 and 1.5, thus justifying our hope that it would be of the order of 1. The limit of 1.5 is obtained when μ_s is infinite, and this corresponds to a solid sphere. The limit of 1 is obtained when $\mu_s = 0$, that is the fluid sphere is inviscid.

From Equation (6.8.3) you can see that the rise velocity of the sphere is proportional to its density deficit and inversely proportional to the viscosity of the surrounding material, and neither of these dependences is surprising. From Equation (6.8.4), you can see that the viscosity inside the sphere is not very important: an inviscid sphere rises only 50% faster than a solid sphere. This implies that the main resistance to the sphere's rise comes from the surrounding viscous fluid that it has to push through in order to rise.

With the other factors held constant, Equation (6.8.3) also says that a larger sphere rises faster, in proportion to r^2 . This results from competing effects. On the one hand, the buoyancy is proportional to r^3 if $\Delta\rho$ is held constant. Against this, the resistance is proportional to the surface area, which varies as r^2 . But the resistance is also proportional to the strain rate, which is proportional to v/r , as noted above. Thus a larger sphere generates smaller strain rates at a given velocity, and thus smaller viscous stresses. The net dependence of the resistance is thus on r (Equation (6.8.2)), and the net dependence of the velocity is on r^2 .

Let us now apply Equation (6.8.3) to a mantle plume head with a radius of 500 km (Chapter 11) and a density deficit of 30 kg/m^3 (corresponding to a temperature excess of about 300°C : Chapter 7). Assume a viscosity of the surrounding mantle of 10^{22} Pa s , typical of mid-mantle depths. Then Equation (6.8.3) gives $v = 2.5 \times 10^{-9} \text{ m/s} = 80 \text{ mm/a} = 80 \text{ km/Ma}$. At this rate the plume head would rise through 2000 km of mantle in 25 Ma. Thus we can get a useful idea of how long it might take a new plume head to reach the surface from deep in the mantle. Just as importantly, we know also how this estimate depends on the assumptions we have made, such as that the deep mantle viscosity is 10^{22} Pa s . If this viscosity is uncertain by, say, a factor of 3, then our estimate of the rise time is also uncertain by a factor of 3: it might be anything between about 8 Ma and 80 Ma.

6.8.2 Flow solution [Advanced]

I will present here the rigorous solution for a solid sphere rising through a very viscous fluid. This was first developed by Stokes [4]. Versions of it are presented by Happel and Brenner [3] (p. 119) and Batchelor [2] (p. 230). Their versions are developed in more general contexts for mathematicians and fluid dynamicists. Here I outline an approach that is more direct in the present context.

The situation is sketched in Figure 6.10, which depicts a buoyant solid sphere of radius a rising slowly, with velocity U , through a viscous fluid of viscosity μ . The problem is symmetric about the vertical axis, and it is convenient to use spherical coordinates (r, θ, ϕ) , where ϕ is the azimuthal angle about the axis. Sometimes it is also useful to use the cylindrical coordinates (ϖ, ϕ, z) . I explained in Section 6.6.4 that with axial symmetry it is possible to define Stokes' stream function, Ψ , and that the force balance equations reduce to

$$E^4 \Psi = 0 \quad (6.8.5)$$

where E is a differential operator given by Equation (6.6.14). In spherical coordinates, E has the form

$$E^2 = \frac{\partial^2}{\partial r^2} + \frac{\sin \theta}{r^2} \frac{\partial}{\partial \theta} \left(\frac{1}{\sin \theta} \frac{\partial}{\partial \theta} \right)$$

and $E^4 = E^2(E^2)$.

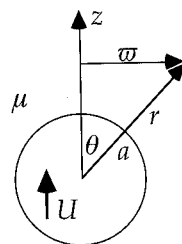


Figure 6.10. Rising buoyant sphere with spherical coordinates (r, θ, ϕ) and cylindrical coordinates (ϖ, ϕ, z) .

The boundary conditions are that the fluid velocity \mathbf{u} equals \mathbf{U} on the surface of the sphere and \mathbf{u} approaches zero at infinity. These can be expressed as follows.

$$\text{At } r = a: \quad u_r = U \cos \theta$$

so

$$\Psi = -0.5 U a^2 \sin^2 \theta \quad (6.8.6a)$$

and

$$u_\theta = -U \sin \theta$$

so

$$\frac{\partial \Psi}{\partial r} = -U a \sin^2 \theta \quad (6.8.6b)$$

$$\text{At } r = \infty: \quad \frac{\Psi}{r^2} \rightarrow 0 \quad (6.8.6c)$$

A common method for solving equations such as (6.8.5) is separation of variables, which can often be used if the boundary conditions are compatible with the solution being a product of separate functions of each independent variable. The spherical geometry suggests using functions of r and θ , and the form of the boundary conditions suggests trying

$$\Psi = \sin^2 \theta F(r) \quad (6.8.7)$$

where F is an unknown function. Substitution into the definition of E^2 above yields

$$E^2 \Psi = \sin^2 \theta \left(F'' - \frac{2F}{r^2} \right) \equiv f(r) \sin^2 \theta \quad (6.8.8)$$

where a prime denotes differentiation and $f(r)$ is another unknown function. Another application of E^2 yields

$$E^4 \Psi = \sin^2 \theta \left(f'' - \frac{2f}{r^2} \right)$$

so from Equation (6.8.5)

$$f'' - \frac{2f}{r^2} = 0 \quad (6.8.9)$$

This equation has a solution of the form

$$f = Ar^2 + \frac{B}{r}$$

so from Equation (6.8.8)

$$F'' - \frac{2F}{r^2} = Ar^2 + \frac{B}{r}$$

This has a particular solution of the form $Ar^4/10 - Br/2$, to which a homogeneous solution of the same form as that for f should be added:

$$F = \frac{Ar^4}{10} - \frac{Br}{2} + Cr^2 + \frac{D}{r} \quad (6.8.10)$$

The boundary condition (6.8.6c) requires $A = C = 0$, while (6.8.6a,b) require $B = 3Ua/2$ and $D = Ua^3/4$. Substitution into Equation (6.8.7) yields finally

$$\Psi = \frac{1}{4} Ua^2 \left(\frac{a}{r} - 3 \frac{r}{a} \right) \sin^2 \theta \quad (6.8.11)$$

From this stream function we can deduce the fluid velocities and other quantities. In particular we want an expression for the viscous resistance to the sphere, and for this it is convenient to have expressions for the pressure and vorticity. The velocities can be found directly from the definition of Ψ in Section 6.6.4:

$$u_r = -\frac{U}{2} \left[\left(\frac{a}{r}\right)^3 - 3\left(\frac{a}{r}\right) \right] \cos \theta$$

$$u_\theta = -\frac{Ua}{4r} \left[\left(\frac{a}{r}\right)^2 + 3 \right] \sin \theta$$

and I also showed there that the ϕ -component of the vorticity is

$$\zeta = \frac{1}{\varpi} E^2 \Psi = \frac{3Ua}{2r^2} \sin \theta \quad (6.8.12)$$

The pressure can be found most easily by putting the force balance equation in the form

$$\nabla p = \mu \nabla^2 \mathbf{u} = -\mu \nabla \times \boldsymbol{\zeta}$$

Substitution from Equation (6.8.12) and integration with respect to r and θ yields

$$p = p_\infty + \frac{3\mu Ua}{2r^2} \cos \theta \quad (6.8.13)$$

where p_∞ is the pressure at infinity.

To get the force on the sphere with minimal manipulation, we need a general result for stresses on a no-slip surface. This is derived in Box 6.B2, where it is shown that the normal and tangential stress components can be written in terms of the pressure and vorticity on the boundary, as given by Equations (6.B2.1) and (6.B2.2). Since these are scalar quantities, the result is independent of the coordinate system, and can be transferred to the surface of the sphere, a portion of which is sketched in Figure 6.11. We want the net force on the sphere in the positive z direction, which we get by adding the z -components of the surface stresses and integrating them over the surface of the sphere. The net z -component is

$$T_z = T_{rr} \cos \theta - T_{r\theta} \sin \theta$$

From the result in Box 6.B2, we get $T_{rr} = -p$ and $T_{r\theta} = \mu \zeta$, noting that the sign of ζ in the $x-z$ coordinates of Figure 6.B2 is opposite to its sign in the $r-\theta$ coordinates of Figure 6.11, assuming that the coordinate systems are right-handed. Substituting for p and ζ from Equations (6.8.12) and (6.8.13), we get the simple expression

$$T_z = -p_\infty \cos \theta - 3\mu Ua/2r^2$$

The net force on the sphere is obtained by integrating over strips of the sphere between θ and $\theta + d\theta$, so that

$$F_z = \int_0^\pi T_z \cdot 2\pi a \sin \theta \cdot a \cdot d\theta$$

with the final result

$$F_z = -6\pi\mu Ua \quad (6.8.14)$$

The contribution from the p_∞ term is zero, as is expected for the net force from a uniform pressure.

This result has the same form as the dimensional estimate, Equation (6.8.2), and they are the same if $c = 3/2$ there, which is

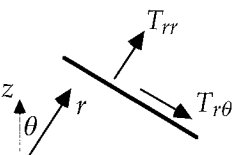


Figure 6.11. Stress components on the surface of a portion of a sphere.

the value obtained from Equation (6.8.4) for a solid sphere. The formula for the velocity of the sphere follows directly as before (Equation (6.8.3)).

The analysis for a fluid sphere proceeds in the same way, except that now a solution for the flow inside the sphere must be matched to a solution for the flow outside the sphere. Thus the boundary conditions are different. The interior and exterior solutions both have the general form given by Equations (6.8.7) and (6.8.10). The calculation of the net force does not simplify in the same way, since the result from Box 6.B2 does not apply in this case. A derivation is given by Batchelor [2] (p. 235).

Box 6.B2 Stresses on a no-slip boundary

The result we need is most easily obtained in Cartesian coordinates, as sketched in Figure 6.B2. From the boundary condition, you can see that the strain component $s_{xx} = \partial u_x / \partial x = 0$. From the conservation of mass for an incompressible fluid, this implies also that $\partial u_y / \partial y = s_{yy} = 0$ on the boundary. Then from the constitutive relation for a viscous fluid,

$$T_{yy} = -p + 2\mu s_{yy} = -p \quad (6.B2.1)$$

From the boundary condition, we also have that $\partial u_y / \partial x = 0$, so that $s_{yx} = 0.5 \partial u_x / \partial y$. But also, the vorticity is

$$\zeta = \left(\frac{\partial u_y}{\partial x} - \frac{\partial u_x}{\partial y} \right) = -\frac{\partial u_x}{\partial y}$$

Then the shear stress component becomes

$$T_{yx} = 2\mu s_{yx} = -\mu \zeta \quad (6.B2.2)$$

Thus on the no-slip boundary, the normal and tangential stress components take the simple forms (6.B2.1) and (6.B2.2).

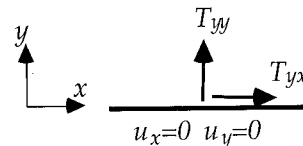


Figure 6.B2. Stress components on a no-slip boundary.

6.9 Viscosity of the mantle

There are a number of observations that indicate that on geological time scales the mantle deforms like a fluid, and these can be used

also to deduce something about the relevant rheological properties of the mantle. Usually it is assumed that the mantle is a linear viscous fluid, and the material is characterised in terms of a viscosity. In Chapter 3 I discussed the origins of the idea that the mantle is deformable, which came particularly from evidence from the gravity field that the earth's crust is close to a hydrostatic (or isostatic) balance, on large horizontal scales, as would be expected if the interior is fluid. I briefly mentioned there that by the 1930s observations of the upward 'rebound' of the earth's surface after the melting of ice-age glaciers had been used to estimate the viscosity of the mantle. This approach, and results from recent versions of it, will now be presented. I will also discuss constraints from the gravity field over subduction zones and from small variations in the earth's rotation. The former provides some additional constraints on the variation of viscosity with depth.

6.9.1 Simple rebound estimates

The land surfaces of Canada and of Scandinavia and Finland (Fennoscandia) have been observed to be rising at rates of millimetres per year relative to sea level. The main observation on which this inference is based is a series of former wave-cut beach levels raised above present sea level. These have been dated in a number of places to provide a record which is usually presented as relative sea level versus time, an example of which is shown in Figure 6.12a.

The inferred sequence of events is sketched in Figure 6.12b. An initial reference surface (6.12b(i)) is depressed a distance u by the weight of glacial ice during the ice age (6.12b(ii)). (The ice load peaked about 18 ka and ended about 10 ka before present.) After melting removed the ice load, the reference surface rose back towards its isostatically balanced level (6.12b(iii)). That rising continues at present with velocity v .

A very simple analysis will illustrate the approach to deducing a mantle viscosity and give a rough estimate of the result. The removal of the ice load generates a stress in the underlying mantle which we can think of for the moment simply as a pressure deficit due to the remaining depression in the earth's surface, which is filled by air or water. This stress is, approximately

$$\tau_p \approx \Delta \rho g u$$

where $\Delta \rho$ is the density contrast between the mantle and the air or water. This stress is resisted by viscous stresses in the mantle.

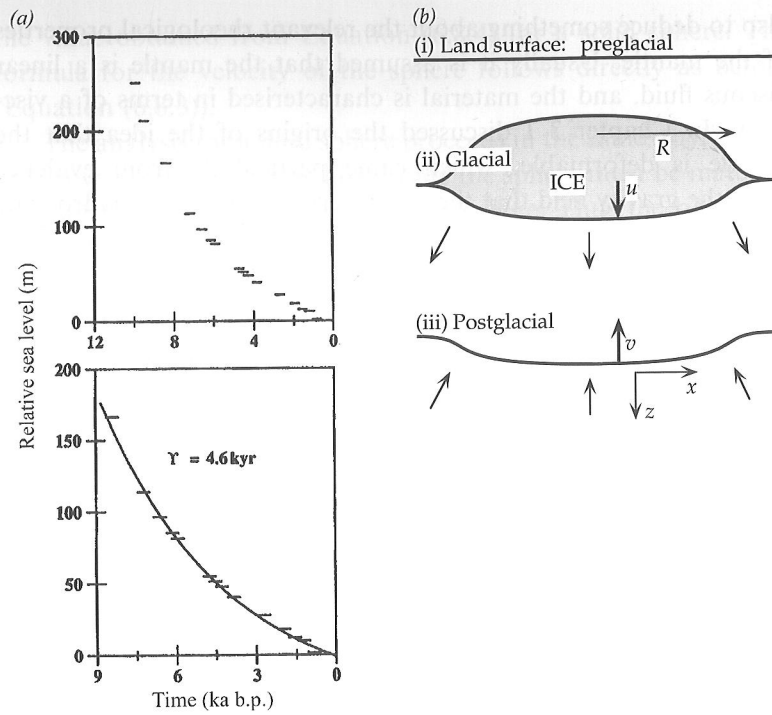


Figure 6.12. (a) Observations of the former height of sea level relative to the land surface at the Angerman River, Sweden. From Mitrovica [5].
 (b) Sketch of the sequence of deformations of the land surface (i) before, (ii) during, and (iii) after glaciation.

Viscous stress is proportional to strain rate, which is proportional to velocity gradient. A representative velocity gradient is v/R , where v is the rate of uplift of the surface and R is the radius of the depression. Thus (compare with Equation (6.5.1)) the viscous stress τ_r will be approximately

$$\tau_r \approx \mu \frac{v}{R} = -\frac{\mu}{R} \frac{\partial u}{\partial t}$$

where the last step follows because v is minus the rate of change of u .

Equating τ_p and τ_r and rearranging gives the differential equation

$$\frac{1}{u} \frac{\partial u}{\partial t} = -\frac{\Delta \rho g R}{\mu} \equiv -\frac{1}{\tau} \quad (6.9.1)$$

where the last identity defines a time scale τ . This has the simple solution

$$u = u_0 e^{-t/\tau}$$

In other words, the depth of the depression decays exponentially with time. The observations of relative sea level fit such an exponential variation well. In Figure 6.12a the decay has a time scale of 4.6 kyr.

This observed time scale can be used in Equation (6.9.1) to estimate a viscosity of the mantle: $\mu = \Delta \rho g R \tau$. Taking $\Delta \rho$ to be 2300 Mg/m^3 , the difference between the densities of water and the mantle, R to be 1000 km and g to be about 10 m/s^2 yields $\mu = 3 \times 10^{21} \text{ Pa s}$. A more rigorous analysis by Haskell [6] in 1937 yielded 10^{21} Pa s . Our estimate here is very rough, but clearly it gives the right order of magnitude, and makes the physics clear.

A more rigorous, though still simplified, analysis can be done by considering a sinusoidal perturbation of the earth's surface. You can think of this as the longest-wavelength Fourier component of the depression in Figure 6.12b, with wavelength $\lambda = 4R$ and wave-number $k = 2\pi/\lambda = \pi/2R$. Thus suppose that after the ice has melted there is a component of the perturbation to the surface topography of the form

$$u(x, 0) = U \cos kx$$

where the coordinates here will be denoted (x, z) , with x horizontal and z vertically downward. The rate of change of this displacement, $v = -\partial u / \partial t$, can be matched by a stream function of the form

$$\psi(x, z) = VZ(z) \sin kx$$

where $V = \partial U / \partial t$ and Z is an unknown function of z . Substitution of this into the biharmonic Equation (6.6.9) then yields

$$\left(\frac{d^2}{dz^2} - k^2 \right)^2 Z = 0$$

which has a general solution of the form

$$Z = a_1 e^{kz} + a_2 e^{-kz} + a_3 z e^{kz} + a_4 z e^{-kz}$$

Requiring the solution to decrease at great depth implies $a_1 = a_3 = 0$. Two other boundary conditions are that the surface

vertical velocity amplitude be V and the horizontal velocity be zero. Using the definition of the stream function (Equation 6.6.7) and application of these conditions then yields

$$\psi = -\frac{V}{k}(1 + kz)e^{-kz} \sin kx \quad (6.9.2)$$

This prescribes everything about the solution to this problem, but relating it to the rebound problem still requires the vertical stress, T_{zz} , at the surface. This stress can be related to the amplitude of the surface displacement, and hence to the restoring stress at the surface, because the high parts exert an excess downward normal stress due to the extra weight of the topography. The low parts exert a (notional) upward normal stress. It is the differences between the weight of the topography in different places that drive the rebound, and these should also match T_{zz} . Thus the stress at $z = 0$ exerted by the topography is

$$W = \Delta\rho g u = \Delta\rho g U \cos kx$$

This must be balanced by the viscous stress, T_{zz} , calculated from Equation (6.9.2). From Equations (6.2.8) and (6.5.4), $T_{zz} = 2\mu s_{zz} - P$. The pressure P can be obtained from the force balance equations, (6.6.5). The calculations are somewhat tedious. It turns out that $s_{zz} = 0$ and

$$T_{zz} = -2V\mu k \cos kx$$

Equating T_{zz} and W ,

$$\frac{\partial U}{\partial t} = -\frac{\Delta\rho g}{2\mu k} U$$

which has the solution

$$U = U_0 e^{-t/\tau}$$

where U_0 is the initial value of U and

$$\tau = 2\mu k / \Delta\rho g = \mu\pi / \Delta\rho g R \quad (6.9.3)$$

This result differs from Equation (6.9.1) by the factor π , and so it will yield a viscosity of $\mu = 10^{21}$ Pa s using the same numbers as used above. This is the same result as obtained by Haskell, even though the problem has been rather idealised.

6.9.2 Recent rebound estimates

A full analysis of postglacial rebound could involve the time and space history of the ice load, the changes in the volume of the oceans as ice accumulates on the continents, the resulting changed magnitude of the ocean load and changed distribution of the ocean load near coastlines, the self-gravitation of the changing mass distributions at large scales, the elasticity of the lithosphere, lateral variations in lithosphere thickness, especially at continental margins, and possible lateral variations in mantle viscosity (e.g. [7]). The full problem is thus very complicated, and has absorbed a great deal of effort.

It turns out that there are certain observations that probe the mantle viscosity more directly, without being greatly affected by the complications introduced by the other factors. One of these is the time scale of rebound at the centre of a former ice sheet after it has all melted. The case in Figure 6.12a is an example of this. Mitrovica [5] has analysed the sensitivity of the inferred viscosity to the ice load history and the assumed thickness of the lithosphere and shown it to be small. He has also analysed the depth-resolution of the observation, that is the sensitivity of the observed rebound time scale to differences in viscosity structure at various depths. This showed that the time scale depends mainly on the average viscosity of about the upper 1400 km of the mantle, a result that is consistent with the intuitive expectation that the deformation due to the ice load will penetrate to a depth comparable to its radius.

The viscosity of 10^{21} Pa s inferred by Haskell from similar data thus represents an average viscosity to a depth of about 1400 km. Mitrovica showed that it is possible for the upper mantle viscosity to be less than the average and the viscosity of the upper part of the lower mantle to be more than the average, with a contrast of an order of magnitude or more, so long as the average value is preserved. Observations from North America support this inference. The North American ice sheet was larger than in Fennoscandia, and hence its rebound is sensitive to greater depth, about 2000 km. A similar analysis of observations from the southern part of Hudson Bay, near its centre, showed that the top of the lower mantle has a higher viscosity. Combining these two analyses suggests a lower mantle viscosity of about 6×10^{21} Pa s and a corresponding upper mantle viscosity of about 3×10^{20} Pa s. Neither of these observations constrains the viscosity in the lower third of the mantle, 2000–3000 km depth, which may be higher still.

These results are consistent with two other types of study, one of geoid anomalies over subduction zones, discussed in the next

section, and the other of postglacial relative sea level changes far from ice sheets. The latter are a second special case that seem to be less sensitive to complicating factors. The idea here is that far from ice sheets relative sea level is controlled not by the ice load, whose effects are negligible, but by changes in the volume of ocean water as ice accumulates on distant continents and then melts again. This causes relative sea level away from the ice loads to be low during glaciations, and to rise as the ice melts, the reverse of the sequence within glaciated areas that is depicted in Figure 6.12a.

It is observed, however, that far from ice sheets the relative sea level rise has not been monotonic, but has overshot by some metres before dropping to present levels. An example is shown in Figure 6.13. The reason for the overshoot is that the ocean basins are not static during the process, because the change in ocean volume changes the load on the sea floor. Consequently, as water is withdrawn the sea floor rises slightly, and as the water is returned it is depressed again. This process happens with a time lag because the mantle is viscous, which means that immediately after all the water has been put back, the sea floor has not completely subsided to its isostatic level, and the water floods slightly onto the continents. Subsequently, as the sea floor completes its delayed subsidence, the water retreats from the continents by a few metres. Thus these so-called Holocene highstands are a measure of the delayed response of the seafloor level to the changing ocean load, and hence

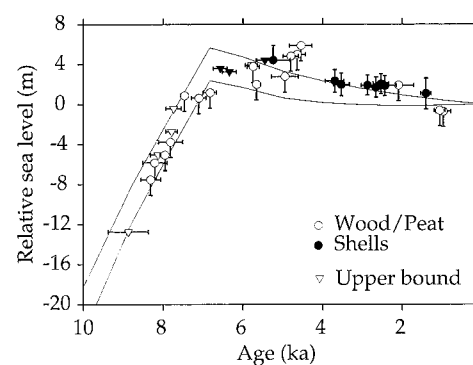


Figure 6.13. Variation of relative sea level with time before present at west Malaysian Peninsula. This example shows a small overshoot of the postglacial rise in sea level, due to the delayed response of the sea floor to the increasing water load. The curves are the envelope of models that plausibly fit the observations from many sites. The steep rise is due to the addition of water until about 7 ka ago, and the subsequent slow fall is due to continued adjustment of the sea floor to the increased water load. From Fleming *et al.* [8]. Copyright by Elsevier Science. Reprinted with permission.

of mantle viscosity [8]. Because the ocean basins are large in horizontal extent, the effects penetrate to great depth in the mantle, and it is expected that the inferred viscosity is an average essentially of the whole depth of the mantle.

Analyses of these observations by Lambeck and coworkers [7, 9, 10] have led to conclusions very similar to those quoted above, a representative result being an upper mantle viscosity of 3×10^{20} Pa s and a lower mantle viscosity of 7×10^{21} Pa s.

So far these approaches have not been combined into a single study of depth resolution, so it is not yet clear whether there is more information to be gained about the lowest third of the mantle. In particular it is not clear whether there is direct evidence for the possibility that the deep mantle has an even higher viscosity, as will be suggested in Section 6.10 on the basis of rock rheology.

6.9.3 Subduction zone geoids

A completely different kind of observation has been used to constrain the relative variation of mantle viscosity with depth, though it does not constrain the absolute values of the viscosity. We saw in Chapter 4 that there are positive gravity and geoid anomalies over subduction zones (Figure 4.9). It was also noted there that the geoid is sensitive to density variations to greater depths than is gravity, and so it is the more useful for probing the mantle. The idea is that these geoid anomalies reflect the presence of higher-density subducted lithosphere under subduction zones. However, the net effect on the gravity field is not as simple as might seem at first sight, because the density variation also causes vertical deflections of the earth's surface and of internal interfaces, which in turn contribute perturbations to the gravity field. The net perturbation to the gravity field depends on a delicate balance of these contributions, and is sensitive to the vertical variation of viscosity in the mantle.

I will explain qualitatively the principles involved in this approach, but without going into details or quantitative analysis. This is partly because the analysis is not simple, and partly because not all aspects of this problem are fully understood at the time of writing. Although the observed geoid can be matched by some models, the accompanying surface perturbations do not match observations as well.

The key physics is shown in Figure 6.14. If there is a high-density anomaly in the mantle, of total excess mass m , then its gravitational attraction will make an extra positive contribution to the geoid. If the mantle were rigid, this would be the only con-

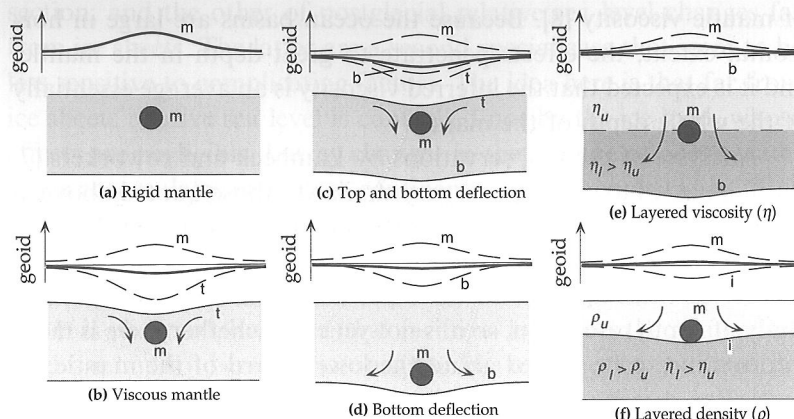


Figure 6.14. Sketches illustrating the ways an internal mass, m , may deflect the top and bottom surfaces or internal interfaces of the mantle, and their contributions to the geoid. Dashed curves are the geoid contributions from mass anomalies correspondingly labelled. Solid curves are total geoid perturbation.

tribution, and the result would be a positive geoid anomaly, as depicted in Figure 6.14a. If however the mantle is viscous, then the extra mass will induce a downflow, and this will deflect the top surface downwards by some small amount (Figure 6.14b). In effect, the viscosity of the mantle transmits some of the effect of the internal load to the surface via viscous stresses. The depression of the surface is a negative mass anomaly (rock is replaced by less dense air or water), and this will make a negative contribution to the geoid. The net geoid will depend on the relative magnitudes of the contributions from the internal mass and from the surface deflection. Actually, both the top and bottom surfaces of the mantle will be deflected, and each deflection will create a negative mass anomaly (Figure 6.14c,d).

The magnitude and sign of the net geoid anomaly depend on the relative magnitudes of the top and bottom deflections, and these depend on the depth of the mass anomaly and any stratification of viscosity or composition that might exist in the mantle. Two principles are at work here. One is that the mass anomalies of the surface deflections balance the internal mass anomaly: it is the same thing as an isostatic balance. The second is that the geoid contribution of a mass anomaly decreases inversely as its distance from the surface. (The geoid is related to gravitational potential, which falls off as $1/\text{distance}$.)

Now if the internal mass anomaly is near the top, then the depression of the bottom surface and its gravity signal are negligi-

ble (Figure 6.14b). The top depression has a total mass anomaly in this case that nearly balances the internal mass, but it is closer to the surface (being at the surface) than the internal mass, so its geoid signal is stronger. Consequently the net geoid anomaly is small and *negative* (Figure 6.14b). This actually remains true for all depths of the internal mass (Figure 6.14c,d), so long as the mantle is uniform in properties, though this result is less easy to see without numerical calculations. It was demonstrated by Richards and Hager [11].

If the lower mantle has a higher viscosity than the upper mantle and the mass is within the lower mantle, it couples more strongly to the bottom surface. As a result, the bottom deflection is greater than for a uniform mantle, whereas the top deflection is smaller (Figure 6.14e). Because the geoid signal from the bottom depression is reduced by distance, it turns out that it is possible for the positive contribution from the internal mass to exceed the sum of the negative contributions from the deflections, and the result is a small *positive* net geoid (Figure 6.14e; [11, 12]).

Richards and Hager [11, 12] also considered the possibility that there is an increase in intrinsic density within the mantle transition zone (Figure 6.14f). The effect of such an internal interface is to reduce the magnitude of the net geoid, because much of the compensation for the internal mass anomaly occurs through a deflection of the internal density interface. Since they are close together, their gravity signals more nearly cancel. The result is that although it is possible for the net geoid to be positive in this case, it is harder to account for the observed amplitude of the geoid anomalies over subduction zones.

A full consideration of subduction zone geoids requires using slab-shaped mass anomalies and spherical geometry, which affects the fall-off of geoid signal with the depth of the mass anomaly. Analyses by Richards, Hager and coworkers [11–14] yielded three important conclusions.

The first is that there is an increase in mantle viscosity with depth, located roughly within the transition zone, by a factor between 10 and 100, with a preferred value of about 30. This is reasonably consistent with the more recent inferences from post-glacial rebound discussed in Section 6.9.2.

The other two conclusions are of less immediate relevance to mantle viscosity structure, but are important for later discussion of possible dynamical layering of the mantle (Chapter 12). The second conclusion is that it is difficult to account for the observed magnitudes of geoid anomalies if there is an intrinsic density interface within the mantle (other than the density changes associated with phase transformations; Section 5.3). The third conclusion is that

subducted lithosphere must extend to minimum depths of about 1000 km to account for the magnitude of the geoid anomalies.

As I noted at the beginning of this section, the geoid does not constrain the absolute magnitude of the viscosity, only its relative depth dependence. This is because the viscous stresses are proportional to the internal mass anomaly, not to the viscosity. A lower viscosity would be accommodated by faster flow, and the stresses would be the same. Consequently the surface deflections would be the same and the geoid analysis would be unaffected. The geoid anomaly depends on the *instantaneous* force balance, into which time does not enter explicitly, rather than on flow *rates*, whereas the glacial rebound effect involves flow rates and time explicitly in the observations and in the physics.

6.9.4 Rotation

The changing mass distribution of the earth during the process of glaciation and deglaciation changes the moments of inertia of the earth, and hence its rotation. Since the mass rearrangements that result from glacial cycles are delayed by mantle viscosity, there is in principle important information about mantle viscosity in these adjustments, and observations do show continuing changes both in the rate of rotation and in the pole of rotation of the earth. A potential advantage of these constraints is that they depend on the largest-scale components of the mass redistribution, and so are sensitive to the entire depth of the mantle.

According to Mitrovica [5], models of these processes are rather sensitive to poorly constrained details of the ice load history and to lithosphere thickness. As well, some models have taken the Haskell viscosity to represent the mean only of the upper mantle, rather than of the upper 1400 km of the mantle, and consequently they do not properly reconcile the two kinds of constraint. At present it is not clear that reliable additional information has been extracted from this approach, but work is continuing.

6.10 Rheology of rocks

Rheology is the study of the ways materials deform in response to applied stresses. Rocks exhibit a range of responses to stress. The response depends on the rock type, temperature, pressure and level of deviatoric stress. It ranges from elastic–brittle near the surface, where pressures and temperatures are low, to ductile or viscous behaviour at the high temperatures and pressures of the interior. The relationship between stress and rate of deformation may be

linear or nonlinear. A linear relationship between stress and strain rate defines a Newtonian viscous fluid. Brittle failure is an example of an extremely nonlinear rheology. It is plausible, though not conclusively demonstrated, that at the low deviatoric stresses associated with mantle convection, the mantle behaves as a linear viscous fluid. However, there is evidence from laboratory experiments that at slightly higher stresses the relationship may become moderately nonlinear.

These features will be briefly summarised here. There are two principal points to be highlighted. First, a brittle–ductile transition occurs in mantle material within depths less than about 50 km. Second, in the ductile range, the viscosity (or effective viscosity in nonlinear flow) is strongly dependent on temperature, changing by up to a factor of 10 for a 100 °C change in temperature. Two other points are also quite significant. The effect of pressure may also be substantial over the depth range of the mantle, and small amounts of water may decrease viscosity by about one order of magnitude.

There remain great uncertainties about the details of mantle rheology. This is because experiments in the pertinent ranges of pressure and temperature are quite difficult, because the time scales and strain rates of the earth are orders of magnitude different from what can be attained in experiments, and because the rheology can be sensitive to the many details of rock and mineral composition and structure, especially to grain size. These uncertainties will be briefly indicated at the end of this section.

6.10.1 Brittle regime

The transition from brittle behaviour near the surface to ductile behaviour at depth in the mantle has a crucial influence on mantle convection that distinguishes it from most other convecting fluid systems, as was indicated in Chapter 3 and will be elaborated in Chapter 10.

I will use the term brittle here loosely for a regime in which deformation is concentrated along faults or narrow shear zones, and in which the behaviour is grossly like that described below using the Mohr–Coulomb theory. As you might expect, the processes controlling failure in aggregates of crustal minerals of a wide range of compositions and in a wide range of conditions are complex [15]. However, a general behaviour emerges in which faults occur and in which they have characteristic orientations relative to the stress field, and these are the essential points I want to present.

Much of the shallow crust is pervasively fractured, but some of it is not, and presumably in the deep crust fractures tend to heal.

Thus we should consider both the brittle failure of intact rock and the sliding of adjacent rock masses along pre-existing fractures. Suppose a piece of rock is subjected to a shear stress, σ_s , and to a confining normal stress, σ_n , as sketched in Figure 6.15a. If there is a pre-existing fracture, suppose that it is parallel to the direction of shearing. Whether there is a pre-existing fracture or not, there is a critical shear stress at which fracture or fault slip occurs, depending either on the strength of the intact rock or on the frictional property of the pre-existing fracture.

It turns out that for either case the shear stress necessary to cause slip is proportional to the normal stress acting across the fault surface. This is in accord with common experience in the case of frictional sliding, in which it is harder to make blocks slide past each other if they are pressed together. Thus we can write

$$\sigma_s = \mu_f \sigma_n + C_f \quad (6.10.1)$$

where μ_f is a coefficient of friction, C_f is a cohesive strength, and σ_s and σ_n are the shear and compressive normal stresses, respectively. Because the engineering convention of considering stress to be positive in tension is unfamiliar and clumsy in this context, I will use the geological convention and notation, in which $\sigma = -T$, which is positive in compression. When applied to frictional sliding with particular values of μ_f and C_f , Equation (6.10.1) is known as Byerlee's rule. When applied to fracture, it is called the Mohr–Coulomb criterion [15]. For my present purpose, it is sufficient to consider C_f to be negligible. Typically $\mu_f \approx 0.6\text{--}0.8$ for rocks.

We can use Equation (6.10.1) to find the orientation in which a new fracture is most likely to occur, or the orientation of a pre-existing fracture which is most prone to slipping. To do this, we need to relate stress components on planes with different orientations. A property of the stress tensor is that there is always an orientation of mutually perpendicular planes on which the shear

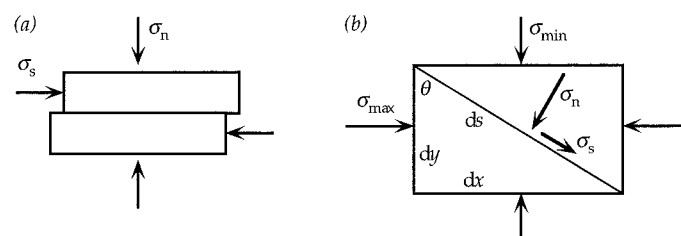


Figure 6.15. Illustration of the relationship between shear stress and normal stress in fracture or frictional sliding.

stresses vanish, leaving three non-zero normal stress components. (If coordinates are defined relative to these planes, the stress tensor contains only the diagonal components. Finding the orientation of these planes is equivalent to diagonalising the stress tensor.) The demonstration of this comes from considering the relationship between stresses on planes of oblique orientation, such as in Figure 6.15b, relative to stresses on coordinate planes. I will not give it here. It can be found in many structural geology and engineering texts, for example. The normal stresses in this orientation are called the *principal stresses*, and they can be arranged in order as the maximum, intermediate and minimum principal stresses.

Figure 6.15b portrays a particular situation that allows us to derive the relationship between the stress components on the oblique plane relative to the maximum and minimum principal stresses. First note that the areas of the orthogonal planes are $dx = ds \cdot \sin \theta$ and $dy = ds \cdot \cos \theta$. Taking the force balance first in the direction parallel to σ_n and then parallel to σ_s yields

$$\begin{aligned}\sigma_n &= \sigma_{\max} \cos^2 \theta + \sigma_{\min} \sin^2 \theta \\ \sigma_s &= (\sigma_{\max} - \sigma_{\min}) \sin \theta \cos \theta\end{aligned}$$

Standard trigonometric identities then yield

$$\sigma_n = \sigma_c + \sigma_r \cos 2\theta \quad (6.10.2a)$$

$$\sigma_s = \sigma_r \sin 2\theta \quad (6.10.2b)$$

where

$$\sigma_c = (\sigma_{\max} + \sigma_{\min})/2$$

$$\sigma_r = (\sigma_{\max} - \sigma_{\min})/2$$

These relationships can be represented geometrically as in Figure 6.16. The stress components on any surface whose normal is oriented at angle θ to the direction of maximum principal stress fall on a circle in this plot, with its centre at the average stress, σ_c , and with radius equal to half the differential stress, σ_r . This circle is known as Mohr's circle.

The Mohr–Coulomb criterion for fracture, Equation (6.10.1), can also be represented on this plot as the sloping line making an angle $\phi = \tan^{-1}(\sigma_s/\sigma_n)$ with the σ_n axis. If the differential stress σ_r is large enough that the Mohr circle is tangent to this line, then the shear stress on a plane with the corresponding orientation is suffi-

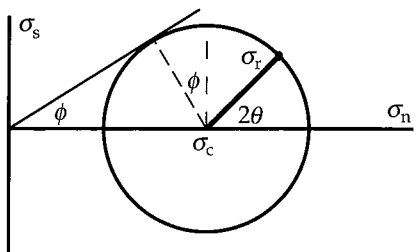


Figure 6.16. Mohr's circle: the geometric representation of stress components on planes with different orientations. The Mohr–Coulomb criterion (Equation (6.10.1)) can also be represented on this diagram by the sloping line (assuming $C_f = 0$).

cient to cause fracture. This tells us that the most likely orientation of a fracture is one whose normal makes an angle such that $2\theta = \phi + \pi/2$ ($\theta = \phi/2 + \pi/4$) with the maximum principal stress direction. It might have been thought that fracture was most likely on a surface with $\theta = \pi/4$, where the shear stress is maximal, but according to this theory the influence of the normal stress component means that a slightly different orientation is preferred, on which σ_n is less. Typically $\phi \approx 30\text{--}40^\circ$, so $\theta \approx 60\text{--}65^\circ$.

This simple theory of fracturing gives a reasonable first-order account both of fracturing observed in the laboratory and of faults observed in the earth's crust. It is found, for example, that normal faults are generally steeper than 45° and reverse faults less steep than 45° , as is expected from this theory. This is explained by Figure 6.17, which shows the expected relationships between maximum or minimum principal stress and the standard fault types of structural geology.

This theory also seems to work for the deeper crust and the mantle part of the lithosphere, even though the rheology there is expected to be more ductile. Evidently deformation is still sufficiently concentrated into narrow shear zones that this theory has some relevance. It is found, for example, that some reverse faults cut completely through the continental crust and into the mantle. It is found also that the major plate boundaries tend to correspond quite well with the standard fault types of Figure 6.17, as discussed in Chapters 3 and 9.

6.10.2 Ductile or plastic rheology

A fairly general relationship for rocks between strain rate, s , and stress, σ , temperature, T , grain size, d , and pressure, P , is [16]

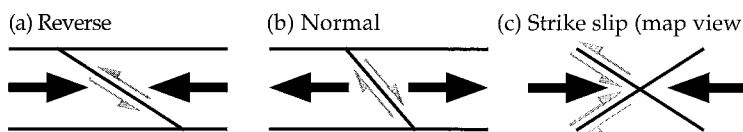


Figure 6.17. Relationship between deviatoric stress in the crust and the principal fault types of structural geology.

$$s = A \left(\frac{\sigma}{G} \right)^n \left(\frac{b}{d} \right)^m \exp \left[- \frac{E^* + PV^*}{RT} \right] \quad (6.10.3)$$

In this equation, A is a constant, G is the elastic shear modulus, b is the length of the Burgers vector of the crystal structure (about 0.5 nm), E^* is an activation energy, V^* is an activation volume and R is the gas constant.

In mantle minerals there are likely to be two main deformation mechanisms. In *diffusion creep*, the deformation is limited by diffusion of atoms or vacancies through grains, and the stress dependence is linear ($n = 1$). There is a strong grain size dependence, with $m = 2\text{--}3$. In *dislocation creep*, the deformation is limited by the motion of dislocations through the grains, the stress dependence is nonlinear ($n = 3\text{--}5$) and there is no grain size dependence ($m = 0$). In each regime there is a strong temperature dependence, but it tends to be stronger in dislocation creep ($E^* = 400\text{--}550 \text{ kJ/mol}$) than in diffusion creep ($E^* = 250\text{--}300 \text{ kJ/mol}$).

Karato and Wu [16] have estimated that in the upper mantle the contributions from the two mechanisms may be of similar order, with one or the other dominating in different circumstances. The lower mantle may be mainly in the linear regime of diffusion creep. Since garnet phases tend to have lower plasticity, it has been suggested that viscosities might be higher within the transition zone. These possibilities must be balanced against the viscosities inferred from observational constraints that were discussed earlier.

There are considerable uncertainties in the absolute magnitudes of the strain rates or apparent viscosities predicted from laboratory data. Nevertheless, an important value of the laboratory work is in establishing the general form of the dependence of the strain rate on state variables and material characteristics. For example, the effect of increasing the temperature from 1600 K to 1700 K is, taking $E^* = 250 \text{ kJ/mol}$ and $R = 8.3 \text{ kJ/mol K}$, to increase the strain rate by a factor of 3. If $E^* = 500 \text{ kJ/mol}$, more appropriate for dislocation creep, the strain rate increases by a factor of 9.

Thus strain rate, and effective viscosity, is strongly dependent on temperature.

For linear rheologies, the viscosity is simply $\mu = \sigma/2s$. From Equation (6.10.3), it is then possible to write the dependence of viscosity on temperature in the form

$$\mu = \mu_r \exp\left[\frac{(E^* + PV^*)}{R}\left(\frac{1}{T} - \frac{1}{T_r}\right)\right] \quad (6.10.4)$$

where μ_r is the viscosity at the reference temperature T_r . Figure 6.18 shows the variation of viscosity with temperature for activation energies of 400 kJ/mol and 200 kJ/mol, assuming the same viscosity of 10^{21} Pa s at a reference temperature of 1300 °C.

The effect of pressure on strain rate is not well understood, because it is hard to reconcile the laboratory and observational constraints. Inferences from postglacial rebound suggest that the deep mantle viscosity is at least one order of magnitude higher than in the upper mantle, but probably not more than three orders of magnitude higher, although this has not been directly tested against the observational constraints. Laboratory estimates are that V^* is about $15\text{--}20\text{ cm}^3/\text{mol}$ for dislocation creep in olivine and about $5\text{--}6\text{ cm}^3/\text{mol}$ for diffusion creep. Even with the latter value, using the pressure of about 130 GPa at the base of the mantle, the predicted viscosity increase is about 12 orders of magnitude over the depth of the mantle. To accord with the observational indications, V^* should be no larger than about $2.5\text{ cm}^3/\text{mol}$.

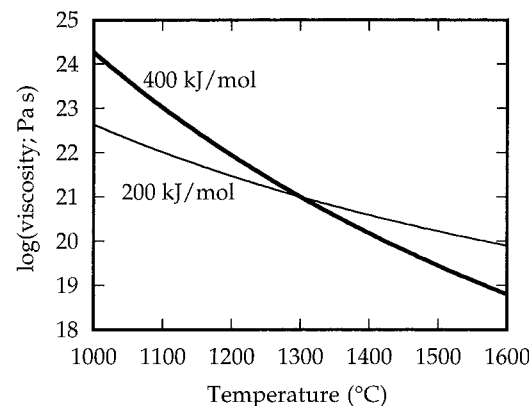


Figure 6.18. Variation of viscosity with temperature for two different activation energies. The viscosity is calculated from Equation (6.10.4), assuming a viscosity of 10^{21} Pa s at a reference temperature of 1300 °C.

Experiments on olivine show that the strain rate increases by more than one order of magnitude if the olivine is water saturated, but the effects of temperature and pressure on this behaviour are not well constrained [16]. Since grain size can be affected by deformation, it is possible that there is a feedback in diffusion creep in which higher strain rates cause smaller grain sizes which in turn cause higher creep rates. Together with the possibility that the non-linear dislocation creep regime is sometimes entered, these possibilities account for a great deal of the uncertainty about absolute strain rates and apparent viscosities in the mantle.

It has been most commonly assumed that the rheology of the mantle is linear. To some extent this is because it is mathematically easier to analyse linear rheology. However, the observational constraints give some support to this approach, though not a compelling argument. If, for example, the rheology were nonlinear during postglacial rebound, then the mantle flow would tend to be more concentrated towards the surface load, and there would tend to be a peripheral bulge developed as mantle was squeezed more to the side than to great depth [17]. This does not appear to have happened, but conclusions from this kind of argument are sensitive to the ice load history and other complications of postglacial rebound.

Whether a linear or nonlinear rheology is assumed, a useful approach is to assume a form like Equation (6.10.3) and combine it with constraints from observations to determine some of the constants, such as A and V^* . This is the approach implicit in Equation (6.10.4). You will see in later chapters that there is a broad consistency between inferences from observations, the general linear form of Equation (6.10.3), and the basic features of mantle convection. In this book only the most basic points are being addressed, and this simple approach is therefore taken. However, mantle rheology must be recognised as one of the main uncertainties in considering mantle convection.

6.10.3 Brittle–ductile transition

The transition between brittle behaviour and ductile or malleable behaviour will occur when ductile deformation can occur fast enough to prevent the stress from becoming large enough to cause brittle failure. Since ductile deformation rates in particular are so dependent on conditions, there is no unique stress, temperature or pressure at which this will occur. Nevertheless it is useful to show some representative examples, with the understanding that other conditions would give significantly different results.

There is a problem in comparing two such different rheological responses. One approach is to plot the differential stress ($\sigma_{\max} - \sigma_{\min}$) that the material can sustain under particular conditions. Then the behaviour that can sustain the least stress is the one that will prevail. Figure 6.19 shows the ‘strength envelopes’, that is maximum stress versus depth, for representative conditions of oceanic and continental lithosphere [15].

It is necessary to assume a geotherm (temperature versus depth) for each case, and for the ductile deformation a strain rate of $10^{-15}/\text{s}$ is assumed. This is representative of mantle convection strain rates and some lithospheric deformation rates. For the oceanic mantle, a lithospheric age of 60 Ma and a dry olivine ductile rheology are assumed, while for the continental mantle, a wet olivine rheology is assumed. The dashed segment in each is an intermediate ‘semi-brittle’ regime in which deformation is by microscopic fracture pervasively through the material (that is, not concentrated along a fault).

A distinctive feature of the continental envelope is that it is bimodal. This is because the deformation rate of crustal minerals is much greater than that of mantle minerals, so the lower crust deforms much more rapidly and prevents brittle failure. However, the actual deformation rate of the lower crust is quite uncertain, and the limit of brittle behaviour might be between 300 and 600 MPa [15]. These curves indicate that the continental lithosphere

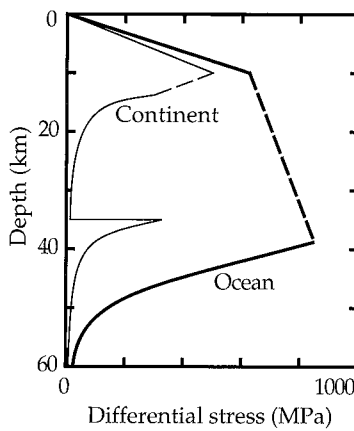


Figure 6.19. Strength envelopes estimated for representative oceanic and continental geotherms. Such estimates depend greatly on details assumed (see text). Each case comprises three regimes: brittle (straight lines), semi-brittle (dashed lines) and ductile (curves). In the continental case, the crustal ductile response changes to the mantle ductile response at 35 km depth. After Kohlstedt *et al.* [15]. Copyright by the American Geophysical Union.

is considerably weaker than the oceanic lithosphere, a fact that seems to be borne out by the observed tendencies of plate boundaries to be diffuse deformation zones within continents, but sharp boundaries within oceans (Chapter 4).

The general relevance of these estimates to mantle convection is that the mantle can be expected to behave as a ductile or viscous material deeper than a few tens of kilometres, but as a brittle material at shallower depths.

6.11 References

1. D. L. Turcotte and G. Schubert, *Geodynamics: Applications of Continuum Physics to Geological Problems*, 450 pp., Wiley, New York, 1982.
2. G. K. Batchelor, *An Introduction to Fluid Dynamics*, Cambridge University Press, Cambridge, 1967.
3. J. Happel and H. Brenner, *Low Reynolds Number Hydrodynamics*, 553 pp., Prentice-Hall, Englewood Cliffs, NJ, 1965.
4. G. G. Stokes, *Trans. Camb. Philos. Soc.* **9**, 8, 1851.
5. J. X. Mitrovica, Haskell [1935] revisited, *J. Geophys. Res.* **101**, 555–69, 1996.
6. N. A. Haskell, The viscosity of the asthenosphere, *Am. J. Sci.*, ser. 5 **33**, 22–8, 1937.
7. K. Lambeck and P. Johnston, The viscosity of the mantle: evidence from analyses of glacial rebound phenomena, in: *The Earth's Mantle: Composition, Structure and Evolution*, I. N. S. Jackson, ed., Cambridge University Press, Cambridge, 461–502, 1998.
8. K. Fleming, P. Johnston, D. Zwart, Y. Yokoyama and J. Chappell, Refining the eustatic sea-level curve since the Last Glacial Maximum using far- and intermediate-field sites., *Earth Planet. Sci. Lett.* **163**, 327–42, 1998.
9. K. Lambeck and M. Nakada, Late Pleistocene and Holocene sea-level change along the Australian coast, *Palaeogeogr., Palaeoclimatol., Palaeoecol.* **89**, 143–76, 1990.
10. K. Lambeck, P. Johnston and M. Nakada, Holocene glacial rebound and sea-level change in northwestern Europe, *Geophys. J. Int.* **103**, 451–68, 1990.
11. M. A. Richards and B. H. Hager, Geoid anomalies in a dynamic earth, *J. Geophys. Res.* **89**, 5487–6002, 1984.
12. B. H. Hager, Subducted slabs and the geoid: constraints on mantle rheology and flow, *J. Geophys. Res.* **89**, 6003–15, 1984.
13. B. H. Hager, R. W. Clayton, M. A. Richards, R. P. Comer and A. M. Dziewonski, Lower mantle heterogeneity, dynamic topography and the geoid, *Nature* **313**, 541–5, 1985.
14. B. H. Hager and R. W. Clayton, Constraints on the structure of mantle convection using seismic observations, flow models and the

- geoid, in: *Mantle Convection*, W. R. Peltier, ed., Gordon and Breach, New York, 657–763, 1989.
15. D. L. Kohlstedt, B. Evans and S. J. Mackwell, Strength of the lithosphere: constraints imposed by laboratory experiments, *J. Geophys. Res.* **100**, 17587–602, 1995.
 16. S. Karato and P. Wu, Rheology of the upper mantle: a synthesis, *Science* **260**, 771–8, 1993.
 17. L. M. I. Cathles, *The Viscosity of the Earth's Mantle*, 390 pp., Princeton University Press, Princeton, 1975.

6.12 Exercises

1. Subscript notation and summation convention: note which of the following expressions are valid, and expand any summations into explicit form. Assume the two-dimensional case (that is, indices running from 1 to 2).
 - (a) $a_i b_j$.
 - (b) $a_{ij} + b_j$.
 - (c) $a_{ij} b_j$.
 - (d) $a + b_i c_i$.
 - (e) $a + b_j c_j$.
 - (f) $a_{ijk} b_k$.
 - (g) $\partial a_i / \partial x_i$.
 - (h) $\partial a_{ij} / \partial x_j$.
 - (i) $\partial a_{ij} / \partial x_k$.
2. Sketch the deformation described by the following displacements and give the values of each component of the two-dimensional strain tensor (Equation (6.3.5)) and rotation tensor (Equation (6.3.6)).
 - (a) $u_x = ay$, $u_y = 0$.
 - (b) $u_x = 0$, $u_y = ay$.
 - (c) $u_x = ay$, $u_y = ax$.
 - (d) $u_x = ay$, $u_y = -ax$.
 - (e) $u_x = ax$, $u_y = ay$.
3. Referring to Figure 6.7, suppose that, instead of the top surface of the fluid layer being a zero-velocity surface, it is a free-slip surface, that is the shear stress is zero on the top surface. Derive the velocity profile in this case, and a formula for the volumetric flow rate.
4. If a mantle plume has a volumetric flow rate of $400 \text{ m}^3/\text{s}$, a radius of 50 km, and a density deficit of 20 kg/m^3 , estimate the viscosity of the material in the plume. Assume that the plume is a vertical cylinder with stationary sides.
5. Calculate the rising or sinking velocity of the following objects.
 - (a) A plume head of temperature excess 300°C and radius 500 km in a mantle of viscosity 10^{22} Pa s .
 - (b) A ‘drop’ of iron of radius 50 km and average density excess 5 Mg/m^3 in a hot mantle with an average viscosity of 10^{20} Pa s . This example gives some quantitative feel for the idea that during the formation of the earth liquid iron would gather into large pools and sink to the core.

6. [Advanced]. Solve for the flow around and within a fluid sphere of viscosity μ_s rising through a fluid of viscosity μ . From this calculate the viscous resistance to the sphere, and its rise velocity. The solutions have the same forms as Equations (6.8.7) and (6.8.10), but the boundary conditions are different. The result from Box 6.B2 does not apply. You can get there with a lot of algebra. Some shortcuts are outlined by Batchelor [2] (p. 235).
7. (a) Complete the steps in the derivation of the stream function solution (6.9.2), that is, show that the general forms assumed are solutions of the relevant equations and that the solution satisfies the boundary conditions. (b) Derive the expression for the normal stress at the surface, T_{zz} , leading to Equation (6.9.3).
8. (a) Calculate a representative strain rate for the mantle assuming the horizontal velocity at the top is 100 mm/a and that it is zero at a depth of 1000 km. (b) From Equation (6.10.3) for the strain rate of a rock, and using the material constants given below, calculate the value of the constant A that would yield the strain rate calculated above. Assume the mantle temperature is 1400°C , the pressure is (approximately) zero, the stress is 3 MPa and the grain size is 1 mm. What is the viscosity? (c) Now calculate the change in viscosity for (i) $T = 1500^\circ\text{C}$, (ii) grain size = 10 mm, (iii) pressure = 30 GPa (equivalent to a depth of about 1000 km).

Material constants: $n = 1$, $\mu_e = 80 \text{ GPa}$, $m = 2.5$, $b = 0.5 \text{ nm}$, $E^* = 300 \text{ kJ/mol}$, $V^* = 5 \text{ cm}^3/\text{mol}$, $R = 8.3 \text{ kJ/mol K}$.